Technical report; TR-215

KNMI

Stratosphere-troposphere exchange of ozone, diagnosed from an ECMWF ozone simulation experiment

Harm Luykx

Koninklijk Nederlands Meteorologisch Instituut

De Bilt, 1998

Technical report = technisch rapport; TR-215

De Bilt, 1998

PO Box 201
3730 AE De Bilt
Wilhelminalaan 10
De Bilt
The Netherlands
Telephone +31(0)30-220 69 11
Telefax +31(0)30-221 04 07

Contact for this report: P. Siegmund

UDC: 551.510.52
551.510.532
551.510.534
551.510.529
551.509.313

ISSN: 0169-1708

ISBN: 90-369-2153-8

Stratosphere-troposphere exchange of ozone, diagnosed from an ECMWF ozone simulation experiment

Harm Luykx

Graduation research project
performed at
the Royal Netherlands Meteorological Institute
Division of Climate Research and Seismology
Section of Atmospheric Composition
De Bilt, The Netherlands

October, 1998

Institute of Marine and Atmospheric Research (IMAU)
University of Utrecht
Princetonplein 5
3584 CC Utrecht
The Netherlands

Abstract

In this study, the stratosphere-troposphere exchange (STE) of ozone has been diagnosed using data from an ozone simulation experiment performed at the European Centre for Medium-range Weather Forecasts (ECMWF). This experiment at the ECMWF started with the implementation of an ozone climatology in the ECMWF model. During the rest of the experiment, the ozone distribution was determined by the model dynamics and a chemistry parameterisation. The present study focuses on a time period of five days of this ozone simulation experiment, from 12 - 17 December 1991.

Besides a diagnosis of the STE of ozone, the dynamical mechanisms responsible for the STE of ozone are described. Also, an overview of estimations of the STE of ozone in the past is presented.

The main goal of this study is to gain insight in the latitudinal dependency of the STE of ozone. For all latitude bands of 2.5° covering the earth, the STE of ozone and the role of the eddies in this exchange are investigated. The global and hemispheric STE of ozone is investigated as well. The STE of ozone is calculated in the extratropics from ozone fluxes across the 3.5 PVU surface, and in the tropics from ozone fluxes across the temperature minimum surface.

The calculated global STE of ozone is $(0.83 \pm 0.34) * 10^4$ kg ozone per second. This value is considerably lower than the mean literature value of about $2.0 * 10^4$ kg ozone per second. This indicates that the method as applied in this study is not sufficiently accurate. An additional calculation of the ozone transport through the 100 hPa surface strengthens this indication.

Most of the latitudinal dependency of the STE of ozone in the Northern Hemisphere can be understood from atmospheric circulation characteristics, such as midlatitude depressions or the subtropical jet. An interpretation of the Southern Hemispheric results, however, is generally less straightforward.

The contribution of the eddies to STE of ozone is small at most latitudes, typically less than 20%. This is mainly due to the low correlation between the STE of air mass and the ozone concentration at the tropopause, which has a mean value of 0.02, with a maximum value of 0.1.

In the method as applied in this study, the ozone flux through the tropopause is generally a small residual of large individual terms. Therefore, the calculated ozone flux is very sensitive to small errors in these individual terms. For this reason, the method as applied in this study is useful for a qualitative diagnosis of the STE of ozone, but not for a quantitative.

Dankwoord

Het afgelopen jaar heb ik afstudeeronderzoek verricht op het KNMI bij de afdeling AS. Ik wil graag een aantal mensen bedanken die mij hebben geholpen in deze tijd. Allereerst mijn directe begeleider op het KNMI, Peter Siegmund, die mij vanaf het begin met veel enthousiasme en inspanning heeft begeleid. Tijdens een aantal tegenslagen die we ondervonden gedurende het onderzoek heeft hij steeds geprobeerd oplossingen hiervoor te vinden en vaak ook gevonden, waardoor mijn onderzoek uiteindelijk tot een goed einde gekomen is. Verder wil ik Geert-Jan Roelofs bedanken die de begeleiding vanuit het IMAU op zich heeft genomen en het verslag heeft nagekeken. Ook wil ik Elias Holm van het ECMWF bedanken. Hij heeft de data aangeleverd waarmee ik mijn onderzoek heb uitgevoerd. Tevens heeft hij gedurende mijn afstudeeronderzoek veel van mijn vragen over de data beantwoord. Hennie Kelder wil ik bedanken voor de mogelijkheid die hij mij heeft gegeven om naar de EGS conferentie in Nice te gaan, wat een geweldige ervaring was. Ik wil de mensen van de afdeling AS bedanken voor de goede sfeer en de belangstelling die ze getoond hebben voor mijn wel en wee tijdens mijn afstudeeronderzoek. Van hen wil ik in het bijzonder Mijke en mijn kamergenote Renske bedanken voor hun belangstelling, ondersteuning en vriendschap tijdens mijn afstudeeronderzoek.

Contents

1. Introduction

Ozone (O_3) plays an important role in the troposphere mainly for two reasons. Firstly, it is important for the chemistry of the troposphere. O_3 is the most important source of OH radicals (Levy,1971). OH reacts with most atmospheric pollutants, and therefore acts as a detergent of the atmosphere. Secondly, particularly in the upper troposphere, ozone acts as a greenhouse gas, thereby influencing the atmospheric radiation budget. Stratosphere-troposphere exchange (STE) of ozone plays a significant role in the budget and distribution of ozone in the troposphere (Roelofs and Lelieveld, 1997). For a better understanding of the tropospheric ozone budget and distribution, it is therefore important to have an accurate estimate of this exchange.

In the past, several methods were used to calculate the STE of ozone. Danielsen and Mohnen (1977), for example, used estimates of the number of tropopause folds per year and mass transport associated with these tropopause folds. They combined this with the correlation between O_3 and potential vorticity (PV). Stratospheric air is characterised by high PV values and tropospheric air by low PV values. The same is true for ozone, so that PV and ozone are positively correlated. Murphy and Fahey (1994) used the almost linear relationship between O_3 and N_2O in the lower stratosphere, in combination with their estimates of upward fluxes of N_2O. These fluxes were estimated from the calculated sink of N_2O, which lies high in the stratosphere. By mass balance, this sink equals the net upward flux of N_2O. Nastrom (1977) computed the average ozone concentration at the tropopause level from a large number of aircraft observations. By using a mean vertical velocity from Angell (1975), he estimated ozone fluxes through the tropopause.

Also, general circulation models (GCMs) have been used to estimate the transport of O_3 from the stratosphere to the troposphere (e.g., Mahlman et al., 1980; Gidel and Shapiro, 1980). Those studies are generally based on fixed PV/O_3 ratios and PV as a tracer. Roelofs and Lelieveld (1997) used a chemistry-general circulation model with sufficiently high spatial and temporal resolution to resolve synoptic disturbances.

New in the present study is the use of meteorological data assimilated by a numerical weather-prediction model to estimate the transport of ozone across the tropopause. In this model, from the European Centre for Medium-range Weather Forecasts (ECMWF), ozone mixing ratios and ozone chemistry have been implemented. Compared with GCMs, numerical weather-prediction models have a greater ability to represent synoptic disturbances (IPCC, 1990, section 4.2.4). Therefore, the transports caused by these disturbances (or transient eddies) are also more pronounced in these models. In case of the ECMWF model, in which ozone is included, this should give more realistic values of the STE of ozone. Moreover, most of the studies on the STE of ozone mentioned above used correlations between ozone and other chemical species or PV. In contrast to these indirect methods, this study uses data from an atmospheric model in which ozone is one of the model variables.

The main goal of this study is to gain insight in the latitudinal dependency of the STE of ozone. For the calculation of the STE of ozone, the method introduced by Wei is used (Wei,1987). Per latitude, the cross-tropopause ozone transport and the dynamic mechanisms (large-scale or small-scale) responsible for this transport are investigated. This is done by decomposing the zonal averaged STE of ozone in a contribution by the zonal mean large-scale circulation, and a contribution by the deviation of this circulation, i.e. the eddies. The former studies on the STE of ozone mentioned above all concern global or hemispheric transports of ozone. For comparison reasons, the STE of ozone through these areas are investigated therefore as well.

In chapter 2 some background on STE will be presented, including the mechanisms responsible for STE. Also, a summary of earlier estimates of the STE of ozone is given. In chapter 3 the data used in this study will be described. A short description is given of the ECMWF model and the way ozone is implemented in this model. In chapter 4 the method used to calculate ozone transport is described. The results of these calculations are given in chapter 5. In chapter 6 the results are discussed, including a discussion about the shortcomings of the Wei-method. Some possible improvements are suggested. Also, in this chapter the conclusions of this study are given.

2. Stratosphere-troposphere exchange of ozone

2.1. Dynamics of stratosphere-troposphere exchange

2.1.1 Large-scale dynamics

At the global scale, STE is realised by a global mean meridional cell, which is called the Brewer-Dobson circulation (Brewer, 1949; Dobson, 1956). This circulation consists of rising cross-tropopause motion in the tropics, followed by meridional drift in the stratosphere towards the winter pole and, finally, downward transport into the extratropical winter troposphere (broad arrows in Fig.1).

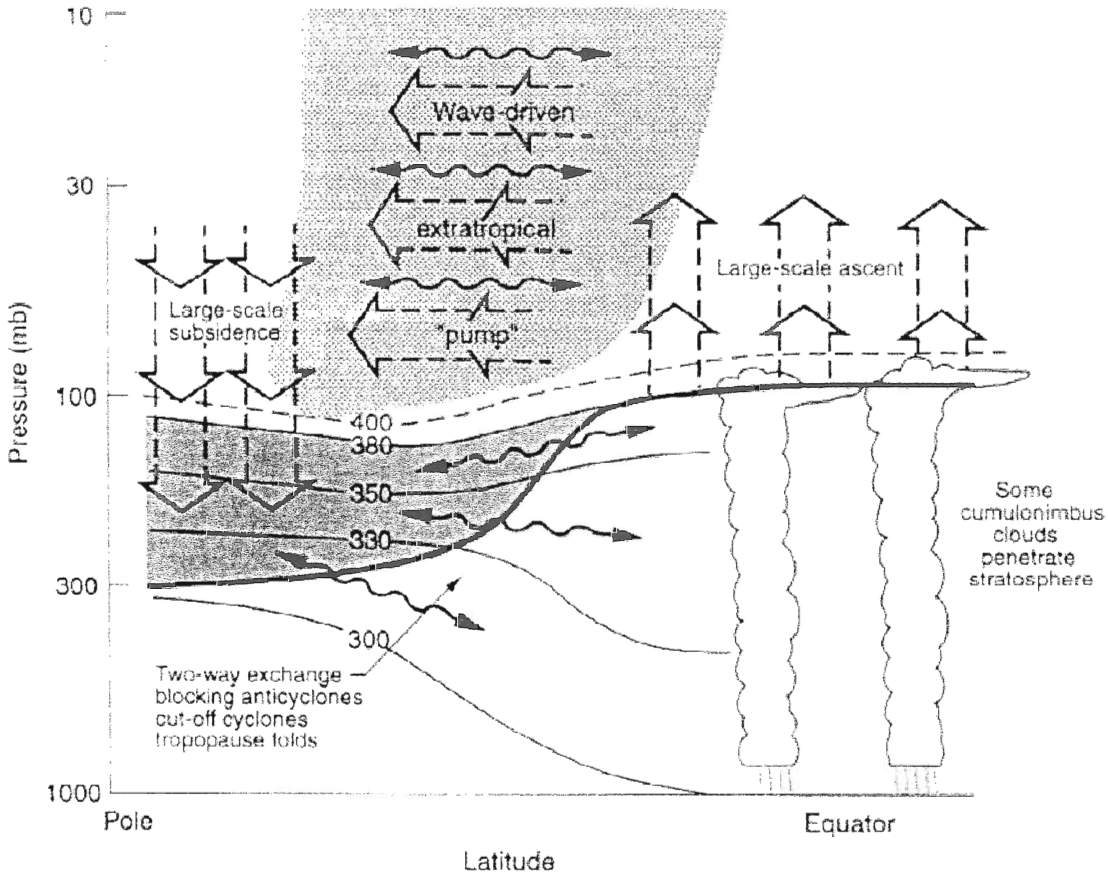

Figure 1: Dynamical aspects of STE. The tropopause is shown by the thick line. Thin lines are potential temperature surfaces in degrees Kelvin. The Brewer-Dobson circulation is denoted by broad arrows. The wiggly arrows denote quasi-isentropic transport by eddy motions. Light shading in the stratosphere denotes the region of the wave-induced westward zonal force. (Holton et al., 1995)

The global-scale circulation drives the stratosphere away from radiative equilibrium conditions due to adiabatic expansion in the rising branch and adiabatic compression in the downward branch. This keeps temperatures below radiative equilibrium in the tropics and above radiative equilibrium in the extratropics. Thus there is a characteristic pattern of radiative heating in the tropics and radiative cooling in the extratropics accompanying the global-scale circulation.

Although the Brewer-Dobson circulation is accompanied by radiative heating and cooling, it is not forced by it. Rather, the upwelling into the stratosphere is a dynamical response to the wave induced zonal force in the extratropical winter stratosphere (light-shaded area in Fig. 1). This force is a consequence of upward propagating Rossby and gravity waves from the troposphere which break in the stratosphere and thereby produce a persistent westward force (Holton et al., 1995). The westward force comes into balance with the coriolis force, which is directed in the opposite direction, thereby causing air to move poleward. Mass continuity now requires a corresponding upward movement of air in the tropical region and a downward movement of air in the extratropics. Thus the heating and cooling patterns observed in the stratosphere do not drive the meridional mass flow, but are a response to it.

2.1.2 Seasonal cycle of STE

The mass transport through the tropopause shows a clear seasonal cycle. In the winter, the wave activity in the troposphere is strongest. As a consequence, the wave induced force in the stratosphere has a maximum in winter too (Holton et al., 1995). This leads to a maximum downward transport in the extratropical stratosphere during winter. In the summer, the tropospheric waves cannot reach the stratosphere (Holton, 1992), so there is no wave breaking in the stratosphere and consequently no wave-induced downward motion in the extratropical stratosphere.

In addition, there is a seasonal cycle in tropopause height. In the northern hemisphere (NH) the tropopause moves upward and poleward from winter to summer, increasing the magnitude of the downward cross-tropopause flux. From summer to winter the opposite happens (Appenzeller et al., 1996).

The combination of these two processes gives a maximum cross-tropopause flux in the late spring and a secondary maximum in midwinter in the NH (Appenzeller et al., 1996). Because the Rossby wave activity in the SH winter is weaker compared to the NH winter, the seasonal cycle is less pronounced in the SH.

The foregoing implies that, globally, the strongest stratospheric downward transport occurs in the NH winter, resulting in a maximum upward mass transport in the tropical stratosphere also in the NH winter. This annual cycle in mass transport in the tropics is consistent with the observed annual temperature cycle near the tropical tropopause. Yulaeve, et al. (1994) showed that this cycle is characterised by temperatures that are several degrees colder in January than in July throughout the tropical lower stratosphere.

2.1.3 Smaller-scale processes

At smaller scales, around the tropopause, transports along isentropes can lead to rapid exchange of air across the tropopause in the extratropics (wiggly arrows in Fig. 1). The smaller-scale processes are associated with synoptic disturbances in the troposphere. Among the processes that can lead to these quasi-isentropic transports are cut-off cyclones and tropopause folds.

The development of cut-off cyclones starts with large latitudinal displacements of the tropopause. These distortions of the tropopause are characterised by tongues of high PV air extending equatorward. Under some circumstances, parts of these tongues roll up to form isolated areas of high PV air referred to as cut-off cyclones (see: figure 2).

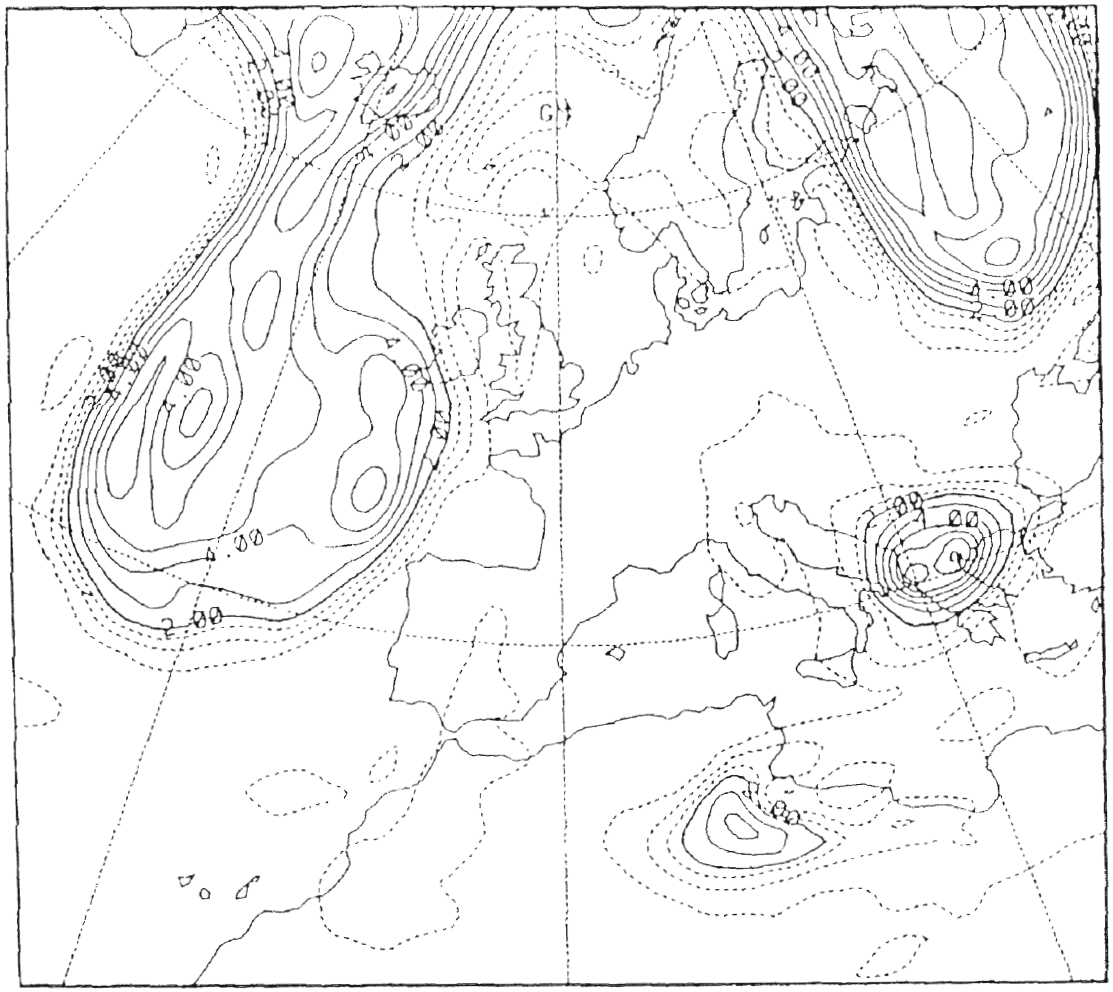

Figure 2: Potential vorticity at the 320 degrees Kelvin isentropic surface. Values are in PVU units (1 PVU = 10^{-6} K m^2 kg^{-1} s^{-1}). The contour interval is 0.5 PVU for the dotted lines and 1 PVU for the solid lines. The air within the solid lines exhibits PV values higher than 2 PVU and denotes stratospheric air. Large latitudinal displacements of stratospheric air are visible above the Atlantic and Russia. Examples of cut-off cyclones are visible above Greece and North-Africa (Holton et al., 1995).

The cut-off lows are characterised by anomalously low tropopause heights. For irreversible transport into the troposphere to occur, nonconservative processes are necessary in order to lower the PV of the air to tropospheric values. Examples of these processes are turbulent mixing followed by diffusion, radiative erosion at the anomalous low tropopause and convectivity. The cut-off cyclone contains cold air originating from the stratosphere. This cold air induces convective instability when the air beneath the cut-off cyclone is warmer, allowing cumulonimbus clouds to enter the stratosphere. This mechanism transports air from the troposphere to the stratosphere. On the other hand, the release of latent heat in the convective motion heats the local tropopause. This lifts the lowered tropopause back upwards, causing air to move from the stratosphere to the troposphere. As shown by Wirth (1998), in a cut-off cyclone, the upward movement of the tropopause is faster than the upward air motion. The net movement of air with respect to the tropopause is therefore downward. Tropopause folds are visible as large vertical deformations of the tropopause directed equatorward and downward into the troposphere (figure 3).

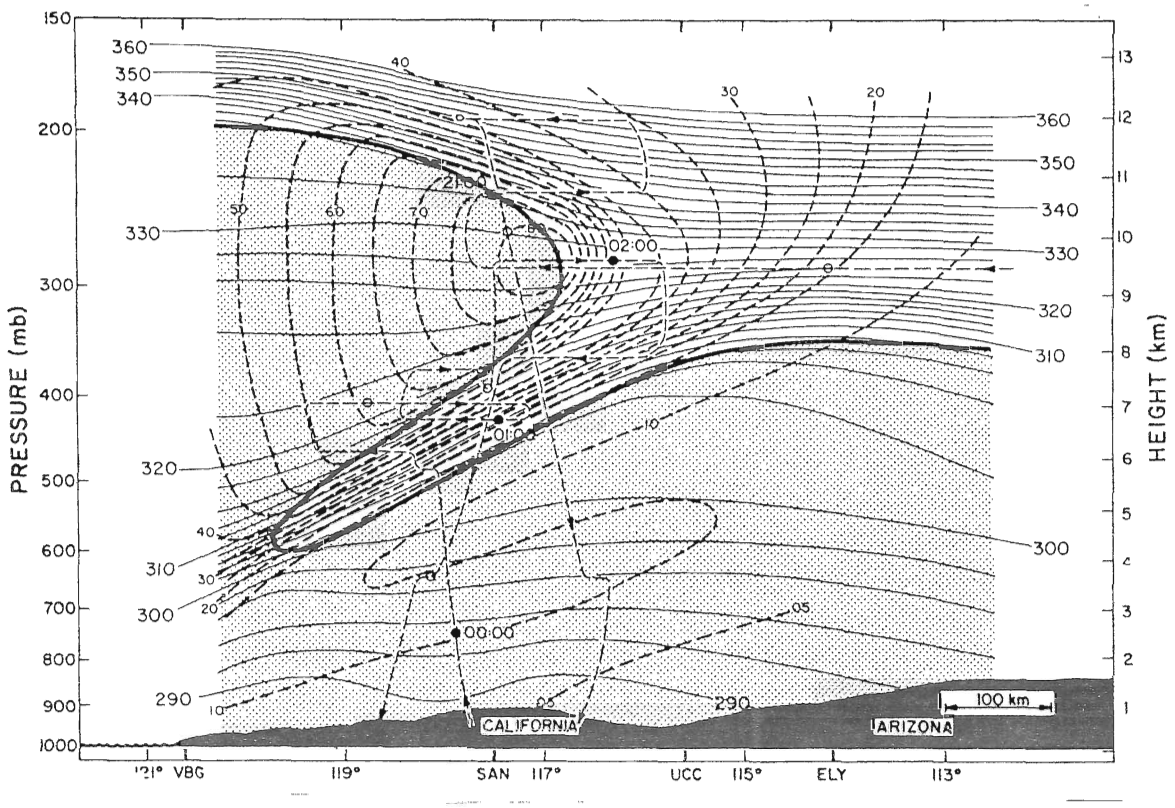

Figure 3: Example of a tropopause fold. Thick solid line denotes the tropopause, thin solid lines denote isentropes, dashed lines denote wind speed contours. The tropospheric air is dashed (Shapiro, 1980).

The development of tropopause folds is associated with upper level frontogenesis and surface cyclogenesis (Vaughan, 1988). The development process is adiabatic, so the descending stratospheric air moves along isentropic surfaces. Again, for irreversible transport into the troposphere to occur, nonconservative processes are necessary. An effective method of exchange in tropopause folds is turbulent mixing at

the edge of the tropopause fold resulting from shear instability of the jet stream (Shapiro, 1980). Not all the air in a tropopause fold is necessarily mixed into the troposphere, a part of it may re-enter the stratosphere before the fold has decayed.

In the tropics, local STE is realised by deep cumulonimbus clouds which penetrate into the stratosphere. However, the total upward transfer of mass is largely independent of the dynamics of the tropical troposphere (e.g., the upward mass transport by convection) (Holton et al., 1995). The exchange rate is ultimately controlled by the large-scale circulation described above and not by tropical cumulus convection. Indeed, on the contrary, the cumulus convection responds to the strength of the large-scale circulation. The large-scale circulation keeps the temperatures below radiative equilibrium at tropopause height, thereby decreasing the tropospheric stability and encouraging deep cumulus convection (Holton et al., 1995).

Although the strength of the large-scale circulation ultimately determines the total mass transport across the tropopause, the smaller-scale processes strongly influence the time and space distribution of such transport. So the processes around the tropopause also strongly determine the latitudinal dependency of STE.

2.2 Stratosphere-troposphere exchange of ozone

2.2.1 Dynamics of the STE of ozone

Most of the atmosphere's ozone is produced in the tropical stratosphere due to the high insolation in that part of the atmosphere. The large-scale circulation, described in the former section, transports this ozone to the extratropical stratosphere where it can enter the troposphere, either by cross-isentropic motion or by motions along isentropes. Because of the vertical gradient in ozone concentration, downward transport of air mass will generally carry more ozone than upward transport of equal air mass. This means that for an estimation of the net ozone transport both the upward and downward air mass fluxes should be known.

The same mechanisms responsible for the seasonal cycle in mass transport through the tropopause are present in the seasonal cycle of ozone transport, leading to a maximum cross-tropopause flux in the spring at both hemispheres, and a minimum in the autumn. In addition, the stratospheric circulation maximum in the winter causes the ozone concentration just above the tropopause to have a maximum around April (Ozon en ultraviolette straling, figure 2.8), thereby contributing to the spring maximum of the STE of ozone. This maximum in ozone flux through the tropopause in spring is a consequence of large-scale phenomena. At smaller scales, most of the ozone exchange from the stratosphere to the troposphere is believed to be associated with tropopause folds (Holton et al., 1995). As is the case for mass transport, synoptic disturbances determine for a large part the location and timing of the cross-tropopause ozone transport, not the total amount (Holton et al., 1995).

2.2.2 Earlier estimates of the STE of ozone

In the past, several estimates of the STE of ozone have been made with different methods (see introduction). An overview of some of these estimates and the methods used is given in Table 1. All numbers are globally integrated transports, unless stated otherwise.

Source	**ozone transport (kg O_3 /s)**	**method used**
Danielsen & Mohnen (1977)	1.5 * 10^4 NH	mass outflow rate estimation based on the measured radioactive tracer ^{90}Sr mixing ratio in tropopause folds and the rate of ^{90}Sr deposition at the ground, combined with the ^{90}Sr-PV-O_3 correlation
Nastrom (1977)	3.2 *10^4	aircraft-measured O_3 concentration around the tropopause and mean vertical velocity (0.5 cm/s)
Gidel & Shapiro (1980)	1.0 * 10^4 NH 0.5 * 10^4 SH	GCM calculation of PV-flux in lower stratosphere combined with PV-O_3 correlation
Mahlman et al. (1980)	3.0 *10^4	GCM with O_3 as an inert tracer. O_3-chemistry at 10 hPa only
Murphey & Fahey (1994)	1.4 * 10^4	calculated upward N_2O flux in the tropical stratosphere combined with N_2O-O_3 correlation
Holton & Lelieveld (1995)	1.7 * 10^4	GCM (10° x 10° x 100 hPa) mass flux calculation and O_3 concentration at 100 hPa
Roelofs & Lelieveld (1995)	1.8 * 10^4	Chemistry GCM (5.6° x 5.6°, 19 vertical layers)
Roelofs & Lelieveld (1997)	1.5 * 10^4	Chemistry GCM (3.75° x 3.75°, 19 vertical levels) with a tracer for stratospheric O_3
Gettelman et al. (1997)	1.6 * 10^4	TEM(1) circulation through 100 hPa and satellite measured O_3 concentration
Tie & Hess (1997)	2.5 * 10^4	3D global chemical transport model

(1) Transformed Eulerian Mean (Andrews & McIntyre, 1976)

Table 1: Global and hemispheric estimates of the STE of ozone.

The different estimates of global STE of ozone show a wide range, varying from 1.4 to 3.2 * 10^4 kg O_3 per second, with an average value of 2.0 * 10^4 kg O_3 per second.

3. Data

To calculate the ozone transports through the tropopause, data calculated with the ECMWF T106L43 prediction model have been used, where T106L43 means that 106 spectral components have been used to span the horizontal plane at 43 levels in the vertical direction. The obtained data have a horizontal resolution of 2.5° x 2.5°. The highest vertical level is at 0.05 hPa, in the mesosphere. Around the tropopause, the vertical resolution varies from about 35 hPa in the polar regions to about 20 hPa in the tropics. The meteorological data consist of vertical wind in pressure coordinates ($\omega \equiv dp/dt$), horizontal wind (u and v), potential vorticity (PV) and temperature (T).

3.1 Ozone in the ECMWF-model

In the ECMWF-model ozone has been implemented for an 80-day ozone simulation experiment that starts at 11 December 1991 (SODA, 1997). This is a part of ongoing work at the ECMWF to improve the representation of the stratosphere in the model.

The first step is the implementation of the zonally symmetric ozone climatology of Fortuin and Langematz (1994) in the model ten days before the simulation starts. Next, the model is integrated ten days forward in time to get a three-dimensional ozone distribution. In this integration, chemistry is not included because apart from the upper stratosphere ozone is dynamically controlled at time scales of ten days. After this integration, the three-dimensional ozone field is normalised by TOMS total ozone to get correct total ozone values at each model column at the starting date of the ozone simulation. In this simulation, the ozone chemistry parametrisation by Cariolle and Déqué (1986) is included but ozone was otherwise left to evolve freely. During the whole experiment, including the 10-day initialisation, the model dynamics were kept close to reality by nudging them towards the known analysed fields for this period.

3.2 Data specification for this study

The data used in this study are ozone and meteorological fields belonging to the first five days of the ozone simulation, starting at 12 December midnight, twelve hours after the beginning of the ozone simulation, and ending at 17 December noon. The time step is 12 hours, giving a time series of ten elements.

4. Method used to diagnose the STE of ozone

4.1 The tropopause

For the method used in this study to calculate the STE of ozone, a unique surface representing the tropopause has to be defined. The tropopause is the surface separating the troposphere from the stratosphere and can be defined using different criteria.

In the extratropics the transition is characterised by a sharp gradient in potential vorticity (PV) which makes it a useful tropopause criterion over there. The values commonly used vary between 1.5 and 3.5 PVU (Potential Vorticity Units, 1 PVU = 10^{-6} K m^2 kg^{-1} s^{-1}). Hoerling et al. (1991) found that the 3.5 PVU value represents an optimal value for tropopause analysis in the extratropics. In the present study, this 3.5 PVU value is also adopted for the extratropics.

In the tropics, PV is not a good criterion because PV vanishes near the equator. Therefore between 10° N and 10° S the temperature minimum is used to define the tropopause. In order to have a smooth transition from the dynamical extratropical tropopause to the thermal tropical tropopause, a combination of both tropopause definitions is used between 30° and 10° at both hemispheres. The tropopause pressure in those areas is determined according to:

$$P_{trp} = WP_{dynamical} + (1-W)P_{thermal} \tag{1}$$

where W is a weight function defined in the NH as:

$$W = 0.5\left(1+\cos\left(\frac{(|\varphi|-30^\circ)}{10^\circ-30^\circ}\right)\pi\right) \tag{2}$$

This weight function equals one at 30N and 30S, and zero at 10N and 10S.

The 3.5 PVU level is determined by going downward from the top level until the first level is reached where the PV is lower than 3.5 PVU. The tropopause pressure is then determined by linear interpolation between this level and the first level above this one.

The zonal and time-mean tropopause pressure for the five days used in this study is depicted in figure 4.

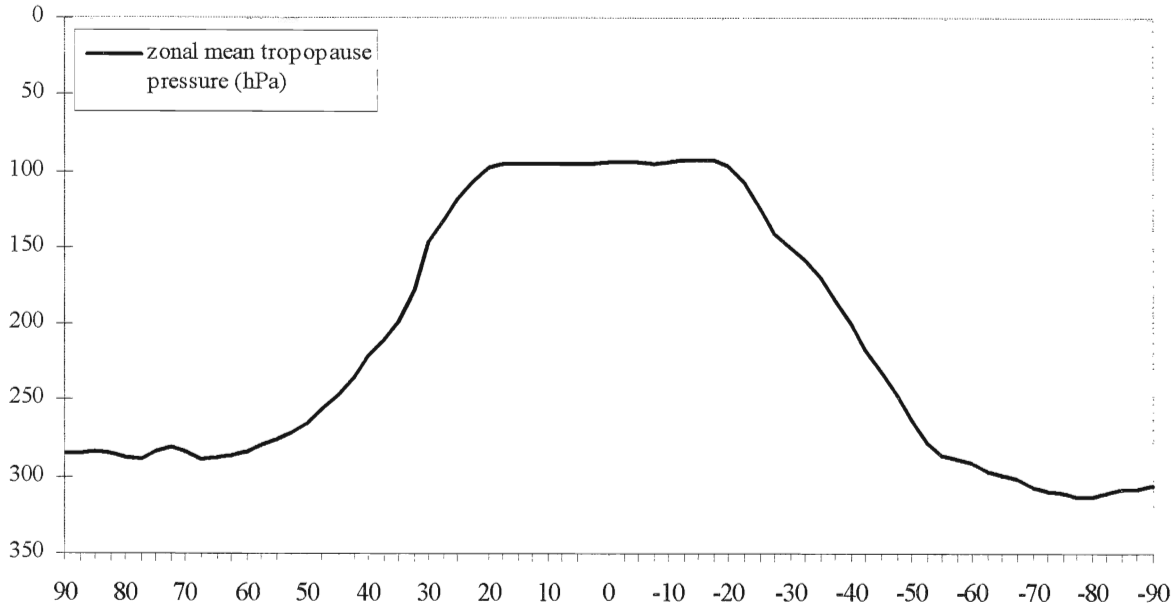

Figure 4: The zonally- and time averaged tropopause pressure, values are in hectopascal (hPa).

4.2 STE of ozone calculation

4.2.1 Method used to calculate the STE of ozone

The STE of ozone is calculated by using Wei's formula in pressure co-ordinates to calculate the ozone fluxes through the tropopause:

$$CTF_{O_3} = O_3\left(\frac{1}{g}(u\frac{\partial p_{tp}}{\partial x} + v\frac{\partial p_{tp}}{\partial y} - \omega) + \frac{1}{g}\frac{\partial p_{tp}}{\partial t}\right) \tag{3a}$$

in short:

$$CTF_{O_3} = O_3 \cdot CTF \tag{3b}$$

where CTF_{O_3} denotes the cross-tropopause ozone mass flux in $kgm^{-2}s^{-1}$ with negative values for fluxes from the stratosphere to the troposphere, CTF the cross-tropopause air mass flux, O_3 the ozone concentration in kg O_3 per kg air, g the acceleration due to gravity, u and v the zonal and meridional wind component, ω (≡dp/dt) the vertical

wind component, p_{tp} the tropopause pressure and $\partial p_{tp}/\partial x$ and $\partial p_{tp}/\partial y$ the pressure gradients along the tropopause. The first two terms on the right-hand side represent horizontal cross-tropopause ozone fluxes due to the skewness of the tropopause relative to the pressure surfaces. The third term represents vertical ozone fluxes through the tropopause. The last term on the right-hand side represents ozone fluxes through the tropopause caused by vertical movement of the tropopause itself.

The three-dimensional wind and ozone values at the tropopause are determined by linear interpolation from the surrounding pressure levels to the 3.5 PVU surface.

To investigate the latitudinal dependency of the STE of ozone, the CTF_{O_3} is integrated over all latitude bands of width 2.5^0 covering the earth.

The STE of ozone is calculated for eight time steps. The first and last time element are omitted because the numerical algorithm used to calculate the pressure tendency term (last term on the right-hand side) at these points did not give reliable results. The pressure tendency terms for the other steps in time are calculated as centred differences:

$$\left(\frac{\partial p}{\partial t}\right)_t = \frac{p_{t+1} - p_{t-1}}{2\Delta t} \tag{4}$$

4.2.2 Determination of the role of eddies in the STE of ozone

The zonally integrated STE of ozone per latitude band can be separated into two parts according to the definition:

$$[STEO_3] = [STE][O_3] + [STE'O_3'] \tag{5}$$

where $[STEO_3]$ denotes zonally integrated STE of ozone in kg O_3 per second, $[STE]$ zonally integrated STE of air in kg air per second and $[O_3]$ the zonal mean ozone concentration in kg O_3 per kg air. This definition arises from the decomposition of a quantity X into an zonally integrated part and a deviation from this zonally integrated part, i.e. X = [X] + X'. The first term on the right-hand side of (5) can be seen as the contribution of the mean large-scale circulation to the STE of ozone. The second term on the right-hand side is the covariance between the STE of air and O_3 and denotes the contribution of the eddies to the cross-tropopause ozone transport. This eddy term can be written as:

$$[STE'O_3'] = corr(STE, O_3) \cdot \sqrt{[STE'^2]} \cdot \sqrt{[O_3'^2]} \tag{6}$$

so the eddy term is a product of three terms, respectively the correlation between the STE of air and O_3, the standard deviation of the STE of air and the standard

deviation of O_3. The standard deviations are a measure of the variation of a quantity along a latitude band. Because ozone concentrations are high in the stratosphere and low in the troposphere, it is expected that, at the tropopause, downward transport carries ozone rich air and upward transport carries ozone poor air. The mass transport across the tropopause and ozone concentration at the tropopause are therefore expected to be negatively correlated. This is the motivation of the use of equation (5) to identify the eddy contribution.

The eddies are the sum of stationary eddies and transient eddies. The stationary eddies are the result of zonal asymmetry in the time-averaged STE of ozone. This ozone transport is caused by stationary waves in the atmosphere, which are a consequence of the earth's orography and topography. The stationary eddies are, in general, well simulated by GCMs. The transient eddies represent ozone transport caused by temporary synoptic disturbances which are clearly present in the ECMWF model, but not so much in GCMs.

5. Results

5.1 Global and hemispheric STE of ozone

With the method described above the mean STE of ozone integrated over the entire globe as well as over both hemispheres is calculated in kg/s for the 5-day period. Also, the sensitivity of the STE of ozone to the tropopause PV criterion is investigated. To estimate the statistical significance of the results, the standard deviation of the mean ozone transports (sigma) is calculated. The values of sigma are obtained as the standard deviation in the individual time series divided by the number of elements in the series used, in this case eight. The results are presented in Table 2.

Tropopause	N.H.	S.H.	Global
3.5 PVU	$0.48 \pm 0.19 * 10^4$	$0.35 \pm 0.18 * 10^4$	$0.83 \pm 0.34 * 10^4$
3.0 PVU	$0.48 \pm 0.16 * 10^4$	$0.27 \pm 0.15 * 10^4$	$0.75 \pm 0.28 * 10^4$
2.0 PVU	$0.65 \pm 0.15 * 10^4$	$0.17 \pm 0.13 * 10^4$	$0.82 \pm 0.19 * 10^4$

Table 2: Global and hemispheric mean STE of ozone (kg/s) and sigma for the five-day period for three different tropopause criteria.

The global STE of ozone is calculated using data valid for the period 12 - 17 December 1991 and can therefore at best be regarded as representative for December, which makes comparison with yearly averaged values difficult. However, according to Tie & Hess, the averaged December STE of ozone is almost equal to the yearly averaged value (Table 1a, Tie & Hess). The global values obtained in this study are below the literature values presented in Table 1. In fact, the value of $0.83 * 10^4$ kg O_3 per second is about half as much as the mean literature value. The global STE of ozone is not very sensitive to the different PV-tropopause choices. Also, it can be seen from Table 2 that the global STE of ozone has a large value for sigma. This is due to the fact that the amount of time steps used for this calculation is low and that the standard deviation in the individual time series is high.

For the NH, the ozone transport values increase when the PV-tropopause lowers, although the standard deviations here are large too. The increase cannot be explained by ozone chemistry between the PV levels because ozone is a passive tracer for the time needed to travel from the 3.5 PVU surface to the 2.0 PVU surface. An explanation for the increase in ozone transport is that the 2.0 PVU surface is moving towards the 3.5 PVU surface, thereby changing the mass and thus the amount of ozone between these two surfaces.

In the SH, the STE of ozone is less compared to the NH, which is what one would expect since at the SH the Brewer-Dobson circulation is absent in December

(see section 2). In contrast to the NH, in the SH the STE of ozone decreases when the PV-tropopause lowers, so the opposite happens, the PV surfaces move away from each other. But for the SH, the standard deviations are large too.

The total global STE of ozone in Table 2 is the sum of zonally averaged alternating areas of upward and downward ozone transport. These areas cancel each other out for a great deal, giving high relative standard deviations. So, the fact that globally and hemispheric integrated ozone transports show large variation for this time period of five days does not mean that no general statements can be given about smaller areas. Clear recognisable areas of upward and downward transports are visible in the zonally integrated ozone transport, as will be shown later.

5.2 Latitudinal dependency of the STE of ozone

The STE of ozone per latitude band is calculated for each point in time individually, and then averaged over the whole period of time. The time-averaged STE of ozone per latitude band including sigma is depicted in figure 5. The values of the STE of ozone in the figure are in kg O_3 per second for the area of the latitude band. Negative values mean downward transport. The latitude-axis starts at 90N and ends at 90S.

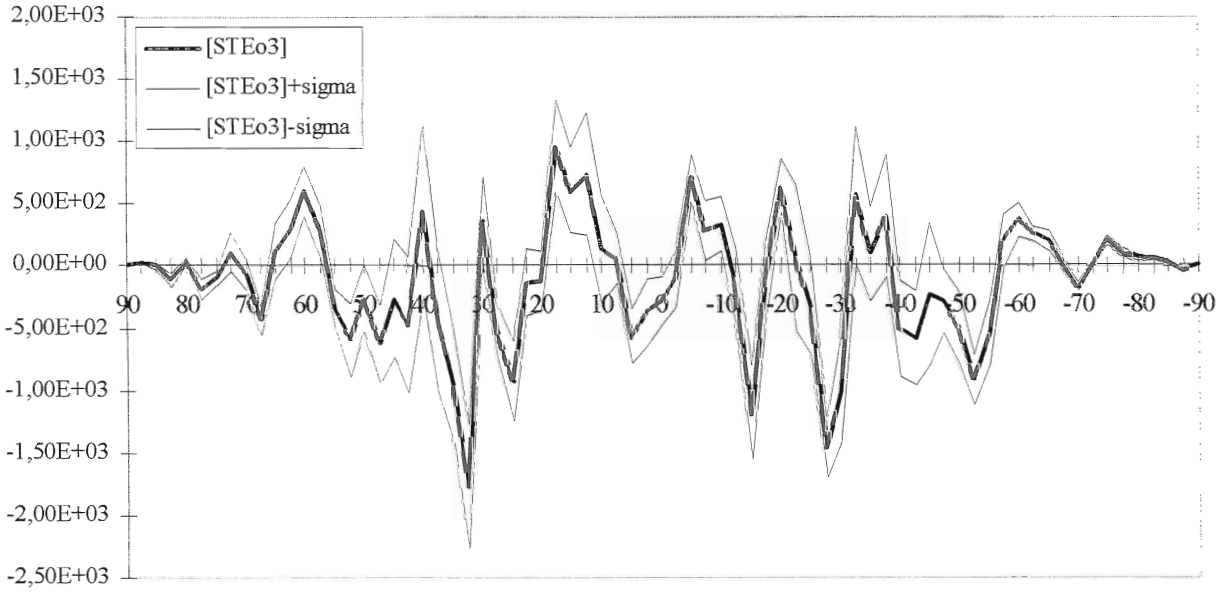

Figure 5: The latitude dependent STE of ozone in kgO_3/s (thick line) +/- sigma (thin lines) calculated per latitude band of width 2.5° for the five day period. Positive values denote upward transport and negative values downward transport.

Starting from the North Pole, an area of significant upward ozone transport through the tropopause is visible between 65N and 57.5N. From here on, significant in this study means that the band between STEO3 + sigma and STEO3 - sigma is either

entirely downward or entirely upward. This phenomenon is also found by Hoerling et al. (1993) for air mass transport through the tropopause in January. They found an area of upward transport between 70N and 50N. An area of significant downward ozone transport is located between 55N and 45N. This area of downward ozone transport coincides with the North-Atlantic and North-Pacific storm track where the STE of ozone is generally caused by tropopause folds associated with synoptic disturbances. The strength of the synoptic disturbances depends on the meridional temperature gradient, which is strongest in winter, hence, ozone transport caused by these disturbances is strongest in winter too. The two peaks of downward ozone transport between 37.5N and 22.5N are most likely associated with the subtropical jet stream, which lies around 30N in the NH winter. In this area, transport across the tropopause occurs irregular and in two directions because isentropes intersect the steep tropopause here. The net transport can therefore either be downward or upward. Because ozone concentrations in the stratosphere are higher than in the troposphere, the net STE of ozone is likely to be downward as is found here. Around 15N, a significant area of upward ozone transport is visible. According to the theory, in the tropics, the net mass transport is upward as part of the large-scale stratospheric circulation. A small area of upward ozone transport is visible around 5S. Around this latitude the upward branch of the ITCZ is located in December. For the rest of the SH until the South Pole, alternating areas of upward and downward transport of ozone are present in figure 5 around about the same latitudes as in the NH. A clear explanation for the location of these areas can not be given. In the SH, less synoptic activity is present compared to the NH. This is because there is less geography and land-sea contrast in the SH. Especially in the SH summer, synoptic activity is low due to the relative weak meridional temperature gradient. Also, the Brewer-Dobson circulation is absent in the SH summer. So one would not expect such high peaks of ozone transport through the tropopause in the SH in December. The succession of positive and negative peaks could point to numerical noise. However, this is probably not the case here because most peaks are significant and present at successive latitudes (for example, the downward peak around 27.5S). The details for the SH are not further investigated in this study.

5.2.1 Sensitivity of the latitude dependent STE of ozone to the PV tropopause criterion

The sensitivity of the STE of ozone for lowering the PV-tropopause to the PV = 2.0 value is investigated for the latitude dependent transport as well. The tropical tropopause between 10N and 10S is unaffected. The results are shown in figure 6.

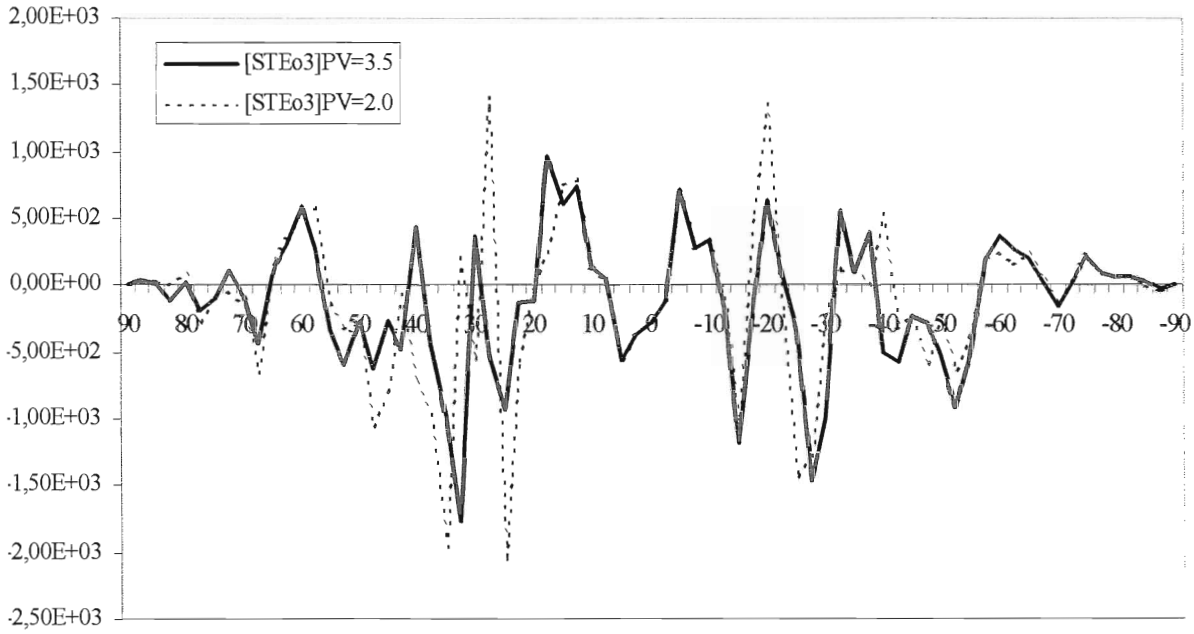

Figure 6: Sensitivity of latitude dependent STE of ozone for two PV-tropopause criteria: PV=2.0 (dotted line) and PV=3.5 (thick line).

Taking the PV value of 2.0 as the extratropical tropopause criterion does hardly change the pattern of upward and downward transport of ozone. Some peaks are shifted and, especially around 30N, are higher. In this area, high peaks of downward and upward transport succeed each other. This irregularity can be explained by the fact that lowering the simulated tropopause will bring it closer to the dynamic active troposphere.

5.2.2 The role of eddies in the latitude dependent STE of ozone

To get more insight in the mechanisms responsible for the latitude dependent STE of ozone, the role of the eddies is investigated. Figure 7 shows the total ozone transport through the tropopause and the components according to equation (5).

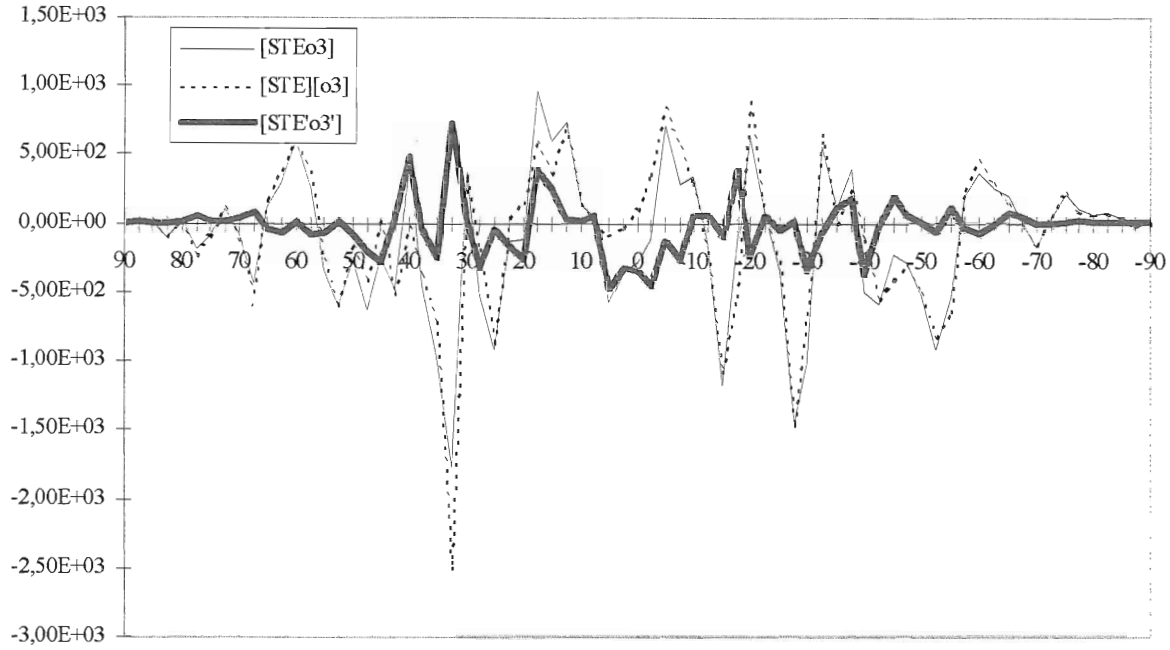

Figure 7: Total STE of ozone (thin line), the component [STE][O_3] (dotted line) and the eddies (thick line). Values are in kg O_3 per second.

One would expect the eddy mechanism to be dominant in the storm track region in the NH midlatitudes. This is not what follows from figure 7. Most of the zonally averaged cross-tropopause ozone transport between 65N and 42.5N is dominated by the product of zonally averaged mass transport and zonally averaged ozone concentrations (dotted line), indicating that the large-scale dynamics are responsible for the STE of ozone in this area. Only in a small area around 45N the eddies are dominant in the downward transport of ozone. The upward transport area around 60N described earlier is almost totally dominated by large-scale transport. In the NH subtropics, two eddy peaks are visible, one at 40N and one at 32.5N, but ozone transport at these latitudes is not significant as can be seen in figure 5. In the tropics between 7.5N and 5S, the eddy transport of ozone is the dominant factor, causing the transport of ozone to be downward in this area. Also, it can be seen from figure 5 that this transport is significant. The reason for this downward ozone transport is not clear. A possible explanation could be that large vertical eddies associated with strong convectivity enter the stratosphere, partly compensated by a return flow which brings back ozone rich air into the troposphere. Just above the tropical tropopause, a strong gradient in ozone concentration is present (figure 8).

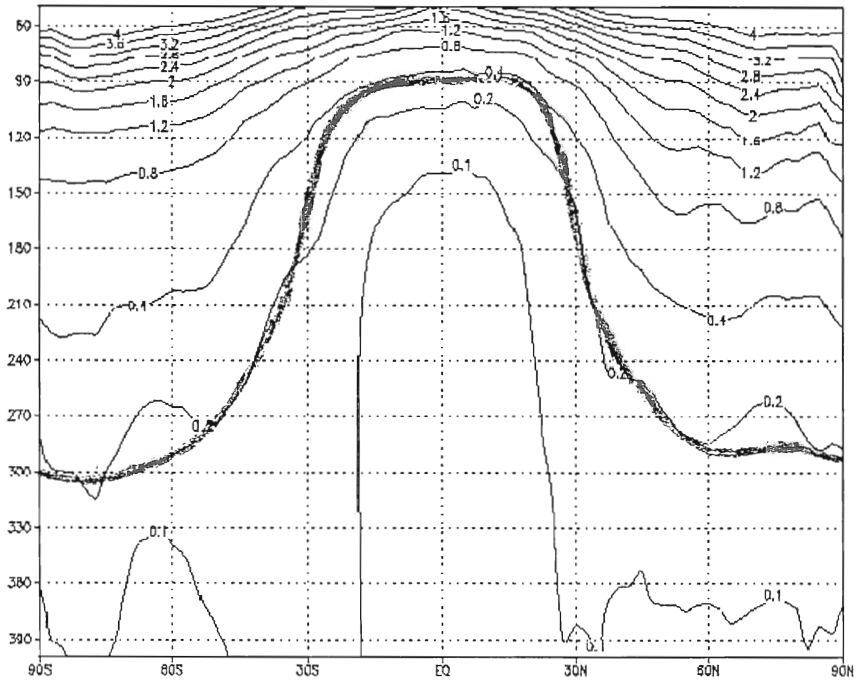

Figure 8: Zonal mean ozone concentration for 11 December in 10^{-6} kgO_3 per kg air. The zonal mean tropopause is denoted by the thick line. The latitude axis starts at 90S and ends at 90N. The vertical axis shows the air pressure in hPa.

Because the calculated eddies are the net result of downward and upward eddies, the downward eddies, transporting ozone rich air, can easily dominate. If this is true, the mass transport and ozone concentration should be significantly negatively correlated.

5.2.3 The correlation between the STE of air mass and ozone concentration

The correlation between the air mass transport (STE) and the ozone concentration (O_3) is depicted in figure 9.

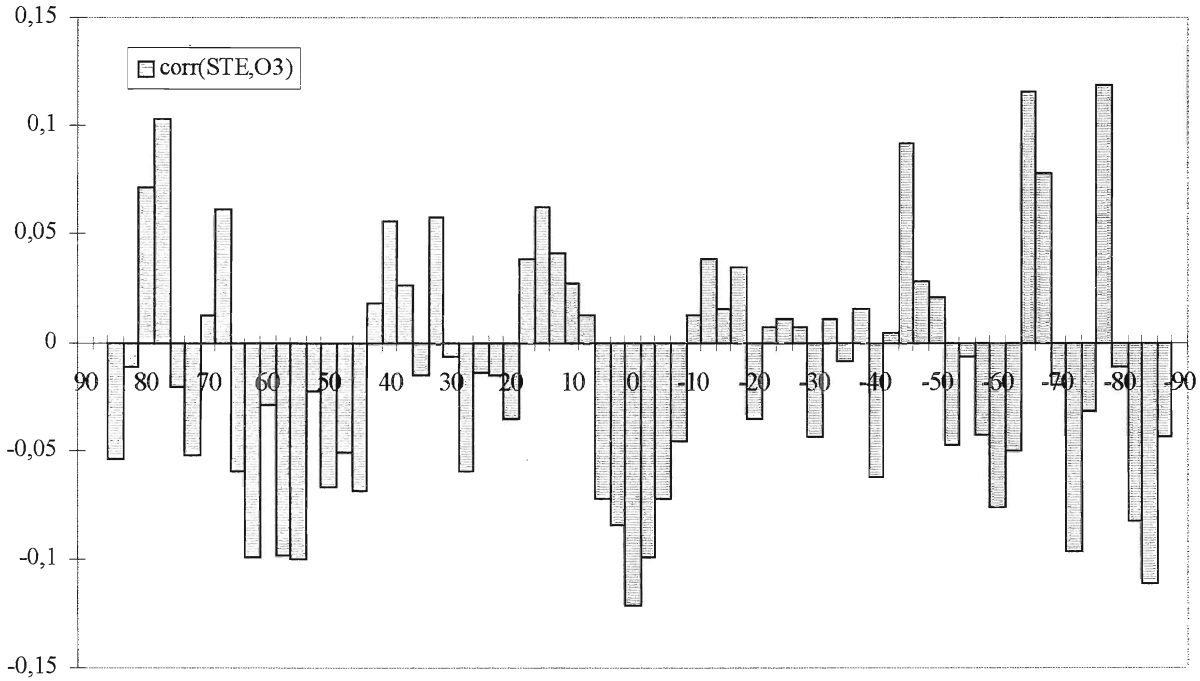

Figure 9: The correlation coefficient between air mass transport through the tropopause and ozone concentrations at the tropopause. Negative values mean that downward transport carries ozone rich air.

What is evident from figure 9 is that the correlation is very low for all latitudes. The highest absolute values lie around 0.1. Apparently, the correlation between the STE of air mass and ozone concentration is not as high as was expected. Even when the variation in the STE of ozone along some latitude bands is high, the net effect can be small due to the low correlation between the STE of air and O_3.

In the tropical area of downward eddy transport, six successive latitude bands with negative correlation between STE and O_3 are present. Taking into account the fact that the correlation is calculated over 144 points in the longitudinal direction and over eight steps in time, this area of six successive negative correlation coefficients is expected to be significant.

In the midlatitudes, between 65N and 45N, nine succesive latitude bands with negative correlation between STE and O_3 are present. Although the eddy contribution at these latitudes is small (see Fig.7), this result satisfies our expectations about downward transport carrying ozone rich air.

5.2.4 Variation in the STE of air mass and ozone concentration along the latitude bands

According to equation (6), the eddies are the product of three terms. If the variation in air mass transport $\sqrt{[STE'^2]}$, and ozone concentration $\sqrt{[O_3'^2]}$ along a latitude band is large, this will be an indication that a large variation in cross-tropopause ozone transport along a latitude band exists, although the zonal mean eddy term contribution may be small. In figure 10, the standard deviation $\sqrt{[STE'^2]}$ and the zonal mean air mass fluxes [STE] are depicted.

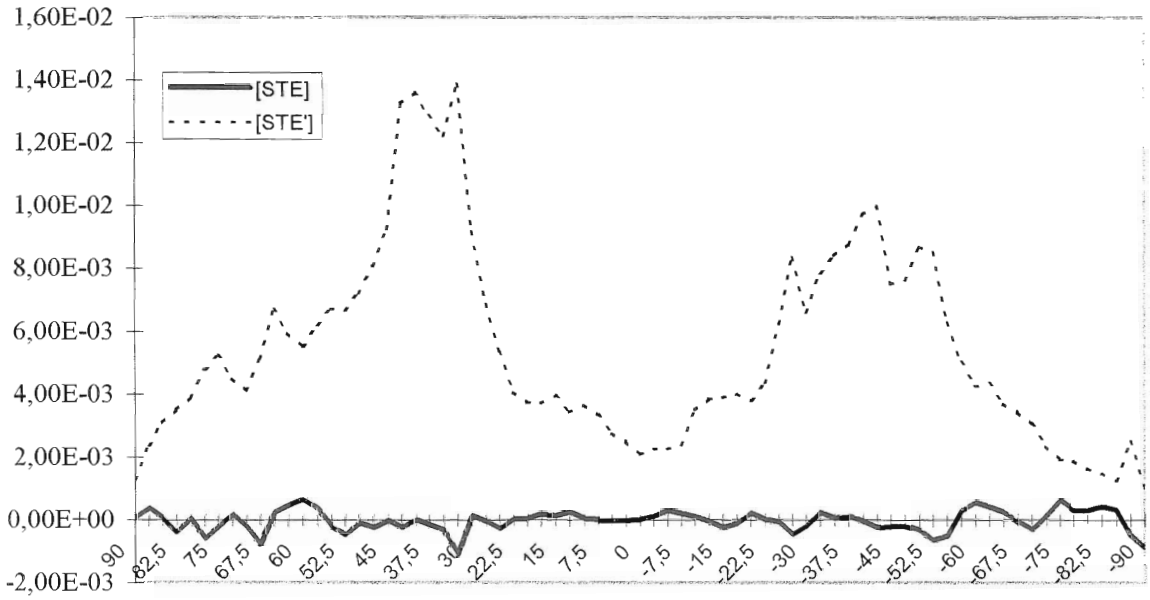

Figure 10: The zonal averaged air mass flux through the tropopause per latitude band in kg/m²s [STE] (thick line) and the standard deviation $\sqrt{[STE'^2]}$ (dotted line).

The standard deviation in the STE of air mass is much larger than the zonal averaged air mass flux. This is due to the fact that the net STE of air mass is the sum of areas of upward and downward transport along a latitude band, giving large variations but small net STE. The areas of largest variations in air mass STE are located in the subtropics and midlatitudes, the areas where the storm tracks and the subtropical jet stream are located.

The same quantities for ozone concentrations at the tropopause are depicted in figure 11.

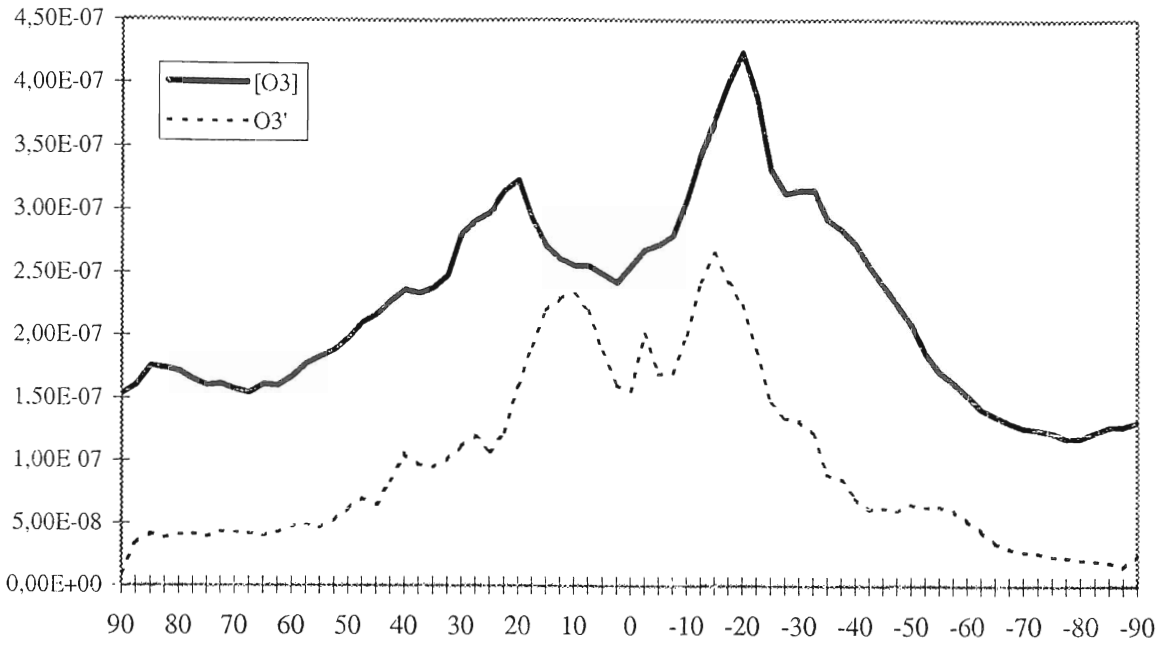

Figure 11: The zonal averaged ozone concentration per latitude band [O_3] (thick line) in kg O_3 per kg air and the standard deviation $\sqrt{[O_3'^2]}$ (dotted line).

This picture is different from figure 10 because ozone concentrations are positive everywhere. The highest zonal mean ozone concentrations are found in the subtropics. The highest variations in ozone relative to the zonal mean are found around the tropics. This is what could be expected since the vertical ozone gradient is high in the tropics. When the local tropopause height is somewhat higher than average, the ozone concentration at the tropopause will be substantial higher. Also, small errors in the determination of the tropopause height can lead to relative large variations in ozone in the tropics. The downward eddy transport of ozone in the tropics is caused by a combination of relative high (negative) correlation and relative high ozone variations.

5.2.5 Two-dimensional distribution of the STE of ozone

To get a clearer picture of how the STE of ozone and ozone itself is distributed at the tropopause, the two-dimensional STE of ozone and the ozone distribution at the tropopause is shown in, respectively, figure 12 and 13. From figure 12 it follows that regions of active STE of ozone can be found in the subtropics and midlatitudes for both hemispheres, coinciding with the storm-track regions and the subtropical jet. Areas of high ozone concentration are mainly found in the tropics and subtropics and not in midlatitudes where they can be expected as a consequence of the synoptic disturbances.

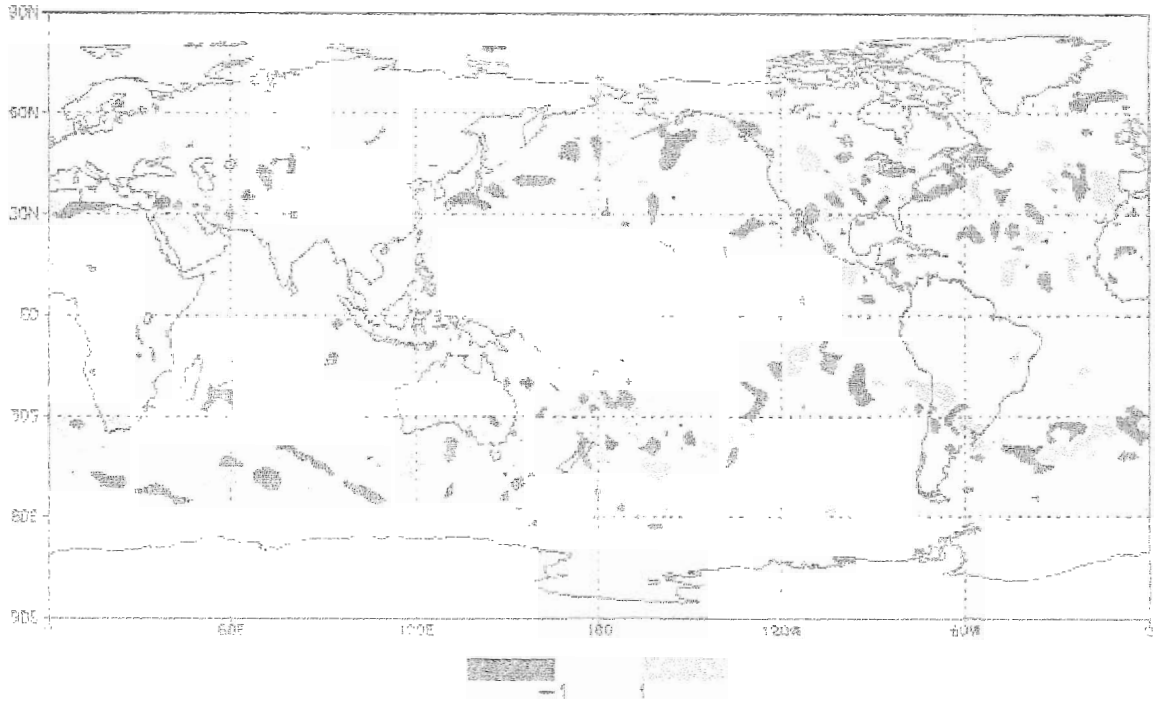

Figure 12: The STE of ozone averaged over five days in 10^9 kg O_3 /m^2s. Positive values (grey areas) denote upward transport, negative values (black areas) denote downward transport.

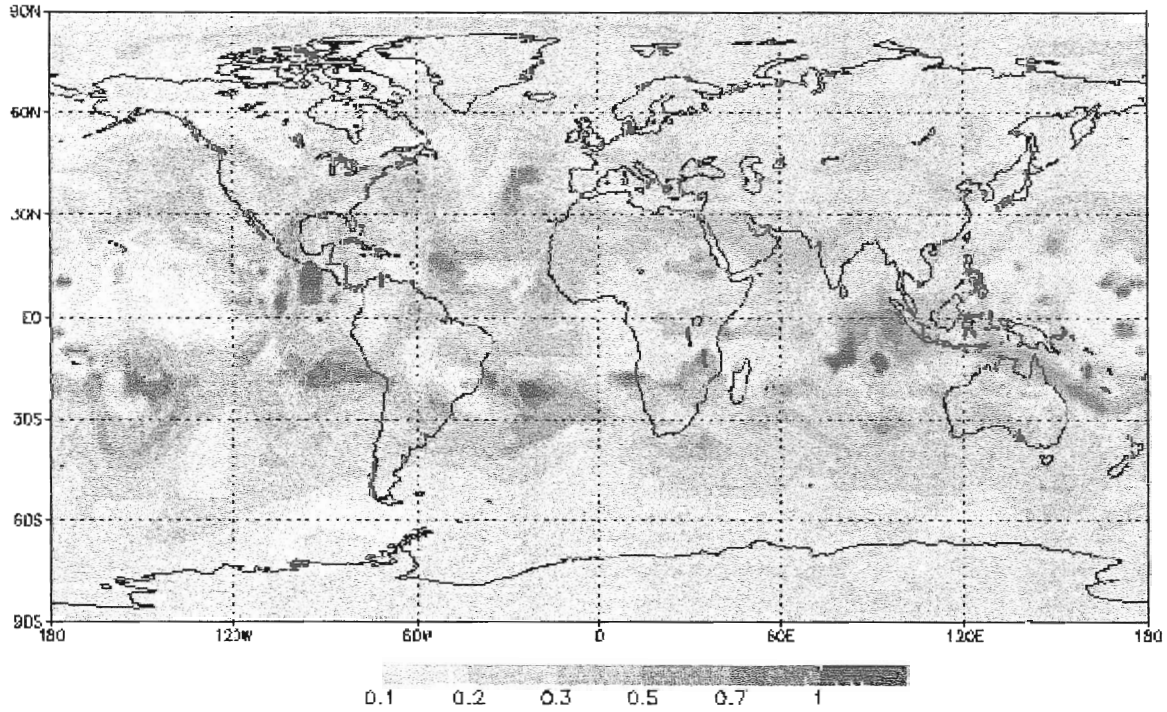

Figure 13: Ozone concentration at the tropopause at 13 December. Values are in 10^{-6} kg O_3 per kg air.

5.2.6 The eddy activity for the individual days

What was clear from section 5.2.2 is that the eddy contribution to the total STE of ozone is small for the time average of five days. It is possible that the eddies are averaged out in time. When at a specific latitude the eddy transport is downward at some time and upward at some other time, the time mean effect could be small. To see if this is true, the eddy contributions of the individual days have been investigated. From this, it could be concluded that the overall picture of low eddy activity remains valid, although some differences are present for the individual days. The most prominent eddy peaks are present at 16 December noon, in contrast to 17 December midnight, when the eddies are generally weak. In figure 14 and 15, [STEO_3] and the components [STE][O_3] and [STE'O_3'] for 16 December noon and 17 December midnight are depicted.

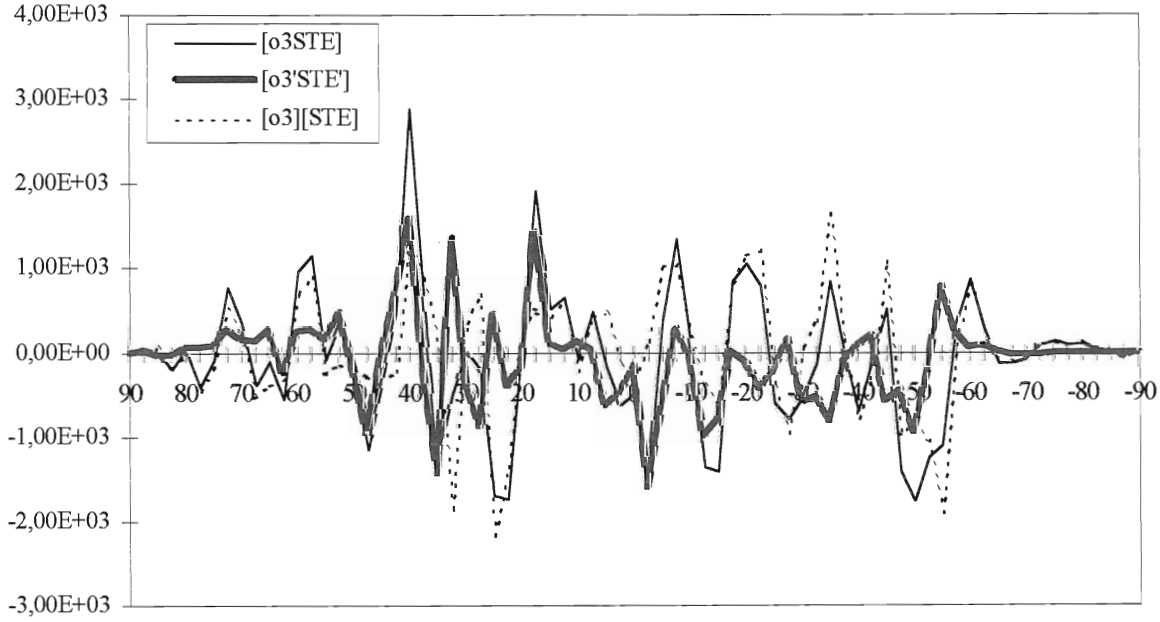

Figure 14: The zonal integrated STE of O_3 and the components [STE][O_3] and[STE'O_3'] for 16 December noon. Values are in kgO_3 /s.

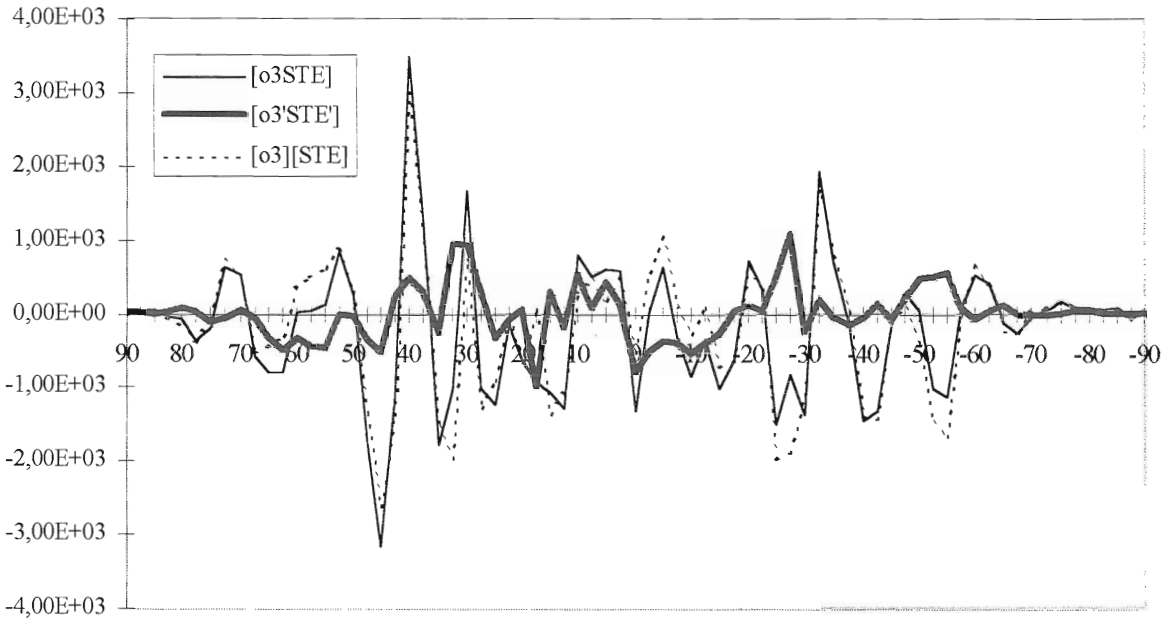

Figure 15: Same as figure 8, but for 17 December noon.

Although the characteristics of the STE of ozone are about the same in both figures, the eddy activity in the NH of the first figure is clearly larger. There, the role of the eddies is dominant at some latitudes. To see what makes up this difference, the three components that determine the strength of the eddies are compared in figure 15 for the area between 70N and the equator.

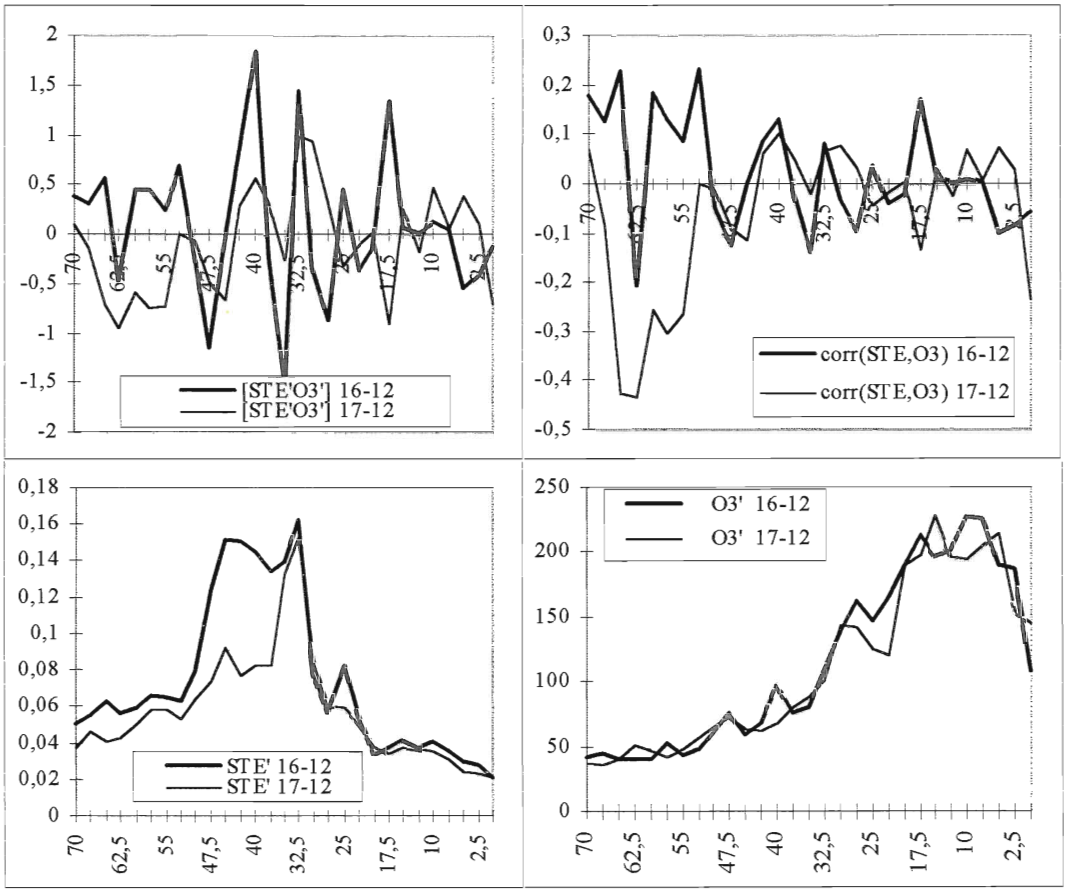

Figure 16: From left top to right bottom, zonal mean eddy terms in kgO_3/m^2s, correlation coefficient between STE and O_3, standard deviation in STE in kg/m^2s and standard deviation in O_3 in 10^{-9} kgO_3 /kg air for 16 December midnight (thick line) and 17 December noon (thin line) between 70N and the equator.

What can be seen in figure 16 is that the high peak around 40N for 16 December is mainly the consequence of the difference in the variation in air mass transport (left bottom) between the two days, the correlation coefficient is small for both at 40N, about +0.1. The peak around 35N is mainly caused by the difference in the strength of the correlation (right top). The same is true for the area of negative eddy transport between 70N and 52.5N for 17 December. Here the correlation is up to -0.4. From this comparison it follows that the strength of the eddies is mainly determined by the strength of the correlation between air mass transport and ozone, although high variation in air mass transport can lead to large eddies even if the correlation is weak.

5.3 Estimation of the magnitude of various relevant terms in the STE of ozone

For a quick overview of the importance of the different terms that determine the STE of ozone (see eqs. 5 and 6), the global estimated order of magnitude of these terms is presented in Table 3.

$\overline{[STEO_3]}$	$\overline{[STE][O_3]}$	$\overline{[STE'O_3']}$	$\overline{[STE]}$	$\overline{[O_3]}$	$\overline{\sqrt{[STE'^2]}}$	$\overline{\sqrt{[O_3'^2]}}$	$\overline{corr(STE,O_3)}$
$3*10^{-11}$	$2*10^{-11}$	$6*10^{-12}$	$1*10^{-4}$	$2*10^{-7}$	$4*10^{-3}$	$8*10^{-8}$	$2*10^{-2}$

Table 3: Magnitude order estimation of the different terms of equation (5) and (6). The overbar denotes globally and time averaged absolute values with $STEO_3$ in units of kgO_3/m^2s, STE in kg/m^2s and O_3 in $kgO_3/kgair$.

From this Table it follows that, globally, the magnitude of [$STEO_3$] is for about two-third determined by the product of [STE] and [O_3]; the eddies play a minor role. The ratio between $\sqrt{[STE'^2]}$ and [STE] is about 40, while the ratio between $\sqrt{[O_3'^2]}$ and [O_3] is about 0.4. For the correlation between STE and O_3, the magnitude order estimation is only 0.02.

The overall conclusion about the role of the eddies in the STE of ozone is that, although the variation in the STE of air mass is high for some latitude bands, the eddy contribution is generally low due to the low correlation between the STE of air mass and the ozone concentration.

6. Discussion and conclusions

6.1 Time period in this study

This study focuses on a time period of five days in December. Only eight points in time were used to calculate the STE of ozone. This was done in order to keep the amount of data manageable. In the calculation of the hemispheric and global STE of ozone, it was seen that sigma was large, in the order of 30% for the global STE of ozone. To get more reliable results, data for a longer period in time are necessary. When averaging over a longer time is performed, for instance a month or a season, stronger statements compared to this study about the STE of ozone for that particular time can be made. If one is only interested in the amount of ozone that enters the troposphere for a large area like a hemisphere, the details around the tropopause are unimportant. For this reason it would be better to look at ozone transports through a pressure surface in the stratosphere, for instance the 100 hPa level. At such a level, the dynamics are much less complicated with a gradual mean downward motion in the extratropical stratosphere as part of the Brewer-Dobson circulation. The ozone flux F_{O_3} across this level is simply given by:

$$F_{O_3} = -\frac{\omega O_3}{g} \tag{7}$$

Ozone is then assumed to be a passive tracer, meaning that ozone that crosses this pressure level is assumed to cross the tropopause at some later time without being affected by chemistry. This is quite a good approximation when no severe heterogeneous chemistry, as is observed over the Antarctic, is present. The global ozone transport averaged over five days through the 100 hPa surface in the present study is (2.8 $\pm$ 0.2) * 10^4 kg O_3 per second. This is about three times higher than was found at the tropopause (Table 2). The 100 hPa value is also within the literature range of Table 1, although it is higher than the average literature value of 2.0 * 10^4 kg O_3 per second. This can be understood by the fact that the Brewer-Dobson circulation is strongest in the NH winter, so the ozone transport through the 100 hPa surface has a maximum in winter too. The observed large difference between the calculated ozone transport through the tropopause and through the 100 hPa surface suggests that the calculated ozone transport through the tropopause is subject to large errors. This could be due to practical difficulties using the Wei-method. In section 6.3, the Wei-method will be discussed.

With respect to the latitude dependent STE of ozone, definite areas of downward and upward transport were found, despite the fact that the time period considered was short. Still, it is not sure if these results will change if longer or other time periods are considered. Therefore one must be cautious to really designate these results as robust. Even if the ozone transport including the spread of plus and minus

sigma is far away from zero, cautioun is required. As a confidence interval around the STE of ozone values, a band of only plus and minus one sigma is taken. There is still a reasonable chance that the STE of ozone for another period of five days differs more than one sigma from the results of this study. Furthermore, the choice of sigma as a measure of robustness is only applicable if the individual events are independent of each other. In this case this means that for a particular latitude, the STE of ozone at one time has to be independent of the STE of ozone at the other times. It has not been investigated if this condition is satisfied. The ozone exchange around the tropopause is an episodic process with a typical lifetime of a tropopause fold of about two or three days. The time resolution in this study is 12 hours. If at one time, strong local cross-tropopause fluxes are present associated with strong synoptic disturbances, these fluxes can still be present 12 hours later in the same latitude band. This makes the two subsequent points in time dependent on each other. Also one could imagine that some synoptic disturbances stay in the same latitude band, some leave the latitude band and others enter the latitude band. Then the total STE of ozone for one latitude band would be quite independent for different points in time and sigma is a good measure for the spread in the latitude dependent STE of ozone. Still, to be able to make general statements about the latitude dependent STE of ozone, a longer time period has to be considered.

6.2 The use of the covariance [STE'O_3'] to identify the eddy activity in the STE of ozone

To determine the role of eddies in the STE of ozone, the statistical definition (5) was used. The eddy contribution was shown to be low for almost all latitude bands. The reason for this was that the correlation between STE and O_3 was low everywhere. This was not expected beforehand. Going from the troposphere to the stratosphere, a sharp gradient in ozone concentration is present with low concentrations in the troposphere and high concentrations in the stratosphere. Thus downward transport should carry ozone rich air and upward transport ozone poor air, giving high correlation between these two. The reason for the low correlation is not clear. The ozone data used in this study are realistic in the sense that ozone concentrations in the stratosphere are much higher than in the troposphere (see figure 8). Although it was shown that the mass transport varies strongly along latitude bands in the subtropics and midlatitudes, the net eddy transport along these latitude bands was low due to the low correlation. For this reason, the statistical decomposition according to equation (5) is only useful to investigate the net eddy contribution to the STE of ozone per latitude band, which is apparently low, meaning that on average the eddies transport about as much ozone upwards as they transport downwards.

The STE of ozone along a latitude band is characterised by regions of strong STE of ozone next to regions of weak STE of ozone. Therefore a two-dimensional framework at tropopause height will give a clearer view of regions of large or small upward and downward transport of ozone compared to the zonal mean framework used in this study. But in a two-dimensional framework, a much longer data set is needed in order to get robust results.

6.3 Comments on the Wei-method

With the Wei formula in pressure coordinates, the ozone flux through the tropopause is calculated as an imbalance of three terms, i.e. the tropopause pressure tendency, the horizontal ozone flux and the vertical ozone flux. The three independent terms do not have any physical meaning concerning STE. The tropopause is a quasi-material surface, meaning that a strong resilience exists for mass to cross the tropopause. In general, the wind blows along the tropopause with just some air passing through the tropopause. For example, when the three-dimensional wind is downward, the tropopause movement will in general be downward too, leading to cancellation between the advective terms and the pressure tendency term. The net cross-tropopause flux is therefore sometimes a small residual of three large terms. Small errors in the individual terms of the Wei-equation can therefore lead to large relative errors in the calculated cross-tropopause flux. When the three-dimensional wind and the pressure tendency terms are zonally- and time-averaged, the possibility of errors due to near compensation is still visible (figure 17).

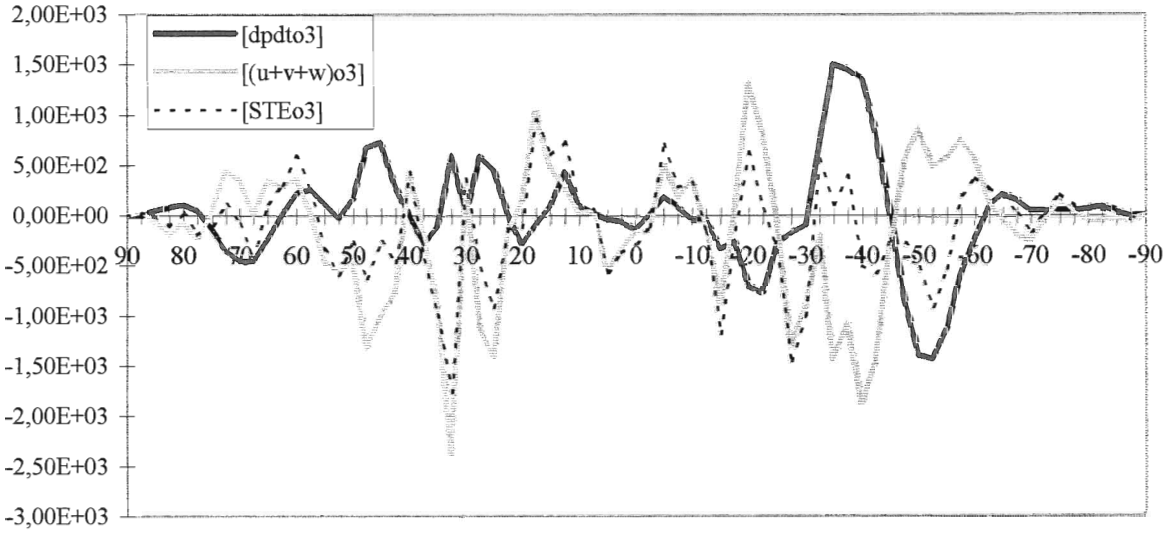

Figure 17: Cross-tropopause ozone transport by tropopause movement (thick line), by total advection (grey line) and the total STE of ozone (dotted line). All values are in kgO_3 per second.

The accuracy of the individual terms strongly depends on the accuracy of the tropopause height determination. Errors in the calculation of the PV field, which determines the tropopause height, could arise from observational or analysis errors. A small error in the calculation of the tropopause height, can have large effects on the pressure tendency term and the horizontal advective term. An erroneous high local tropopause, for instance, can lead to large errors in the horizontal wind component if wind speeds are high. When a strong westerly wind is present, the west side of the erroneous high tropopause will have transport from the stratosphere to the troposphere and the east side transport from the troposphere to the stratosphere. The effect of these errors on the net ozone transport through the tropopause could be small when the fluxes are averaged over space, but this is not certain. When at the

next point in time the calculated tropopause is substantial lower, the pressure tendency term will give erroneous high ozone fluxes from the troposphere to the stratosphere. These errors are not compensated by the vertical wind component because that term is calculated instantaneously. Again, these errors could largely disappear after averaging over space and time. An error in the calculated pressure tendency term without errors in the tropopause height calculation is not unlikely too. The pressure tendency term is calculated as an average over 24 hours, which of course is not necessary equal to the instantaneous value at the middle of this time interval at which point the other terms are determined. This difference in nature between the pressure tendency term, calculated as an average over a period in time, and the advective terms, known at one point in time, is one of the major difficulties in the use of the Wei-method. Siegmund et al. (1996) showed that for the time- and space resolution that they used in their study of cross-tropopause mass transport, a complicated numerical scheme for the calculation of the advective term was necessary in order to avoid erroneously large positive and negative instantaneous fluxes. Such a scheme is needed if the temporal resolution is too low to 'follow' the movements of the smaller structures in the tropopause surface. Compared to this study, their resolution in time was four times higher and their horizontal resolution was five times higher, so the ratio between these two is not much different from this study. The numerical scheme used in their study was not used in this study.

Wirth (1998) examined the STE of mass in a cut-off cyclone using different version of the Wei formula. Besides calculations with the same version used in this study, he calculated the STE with PV as the vertical co-ordinate in the Wei formula. The advantage of using PV as a vertical co-ordinate in a framework in which a unique PV value is taken as the tropopause is that the horizontal flux term and the tropopause pressure tendency term vanish trivially. In this way, the possibility of compensation between individual terms in the Wei equation disappears. In case of ozone fluxes, the Wei formula simply changes to:

$$CTF_{O_3} = O_3 \frac{1}{g} \frac{\partial p}{\partial PV} \frac{dPV}{dt} \tag{8}$$

Disadvantage of this version of the Wei formula is that knowledge of the sources and sinks that determine the PV evolution in time is necessary to be able to calculate the ozone fluxes. With the use of equation (8), Wirth found downward transport of mass in the cut-off cyclone due to diabatic heating (see chapter 2). This downward transport was the sum of a relative small upward contribution and a relative large downward contribution. The same calculations in pressure co-ordinates gave different results with net mass exchange being the sum of successive adjacent areas of large upward and large downward mass transports. When the non-conservative processes were switched off, the mass exchange disappeared in the PV co-ordinate system (by definition), but with pressure as a vertical co-ordinate, the large up- and downward fluxes persisted, leading to a substantial net mass exchange. He concluded that these large up- and downward terms arose from the near cancellation of large individual terms in the Wei formula in pressure co-ordinates and designated them as numerical artefacts. Subsequent areas with large up- and downward transport are present in

this study too. Figure 18 shows the STE of ozone per grid cell along the latitude band around 60N for a particular day.

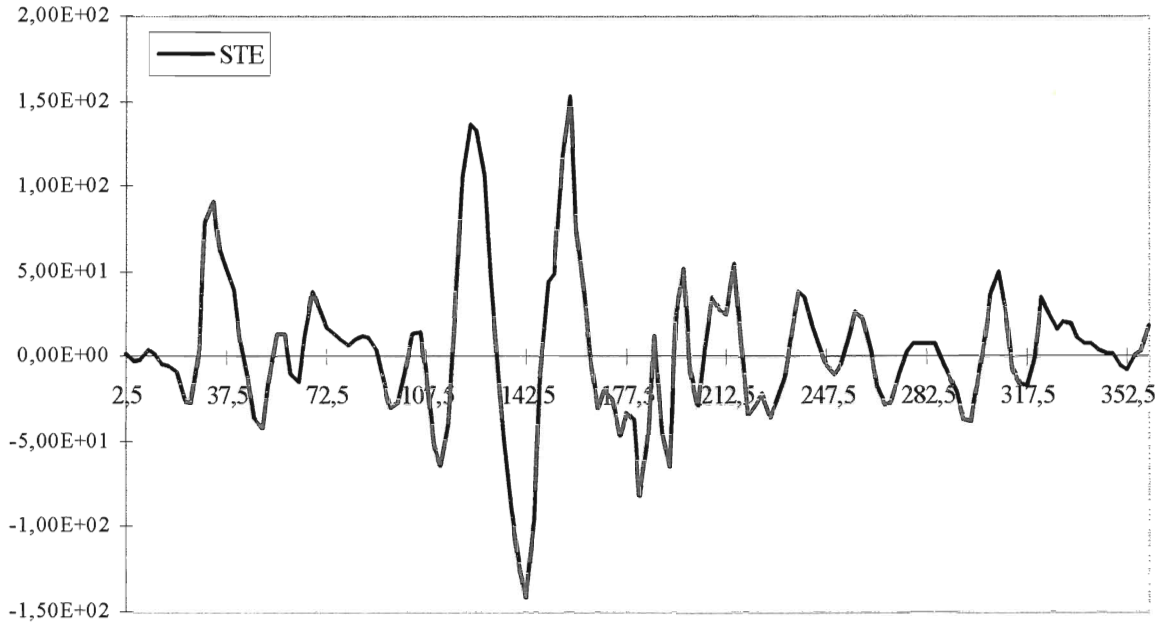

Figure 18: Instantaneous STE of ozone per grid cell of 2.5° x 2.5° along a latitude band around 60N. The longtitude-axis starts at 0° (Greenwich meridian). Values are in kgO_3 per second.

These peaks may thus be caused by the near cancellation between large individual terms in the Wei formula.

The net STE of ozone per latitude band is the sum of these areas of negative STE of ozone and positive STE of ozone along a latitude band. That at some latitudes the net STE of ozone is a small residual of total downward and total upward transport of ozone can be seen in figure 19, which shows the STE of ozone for 14 December midnight.

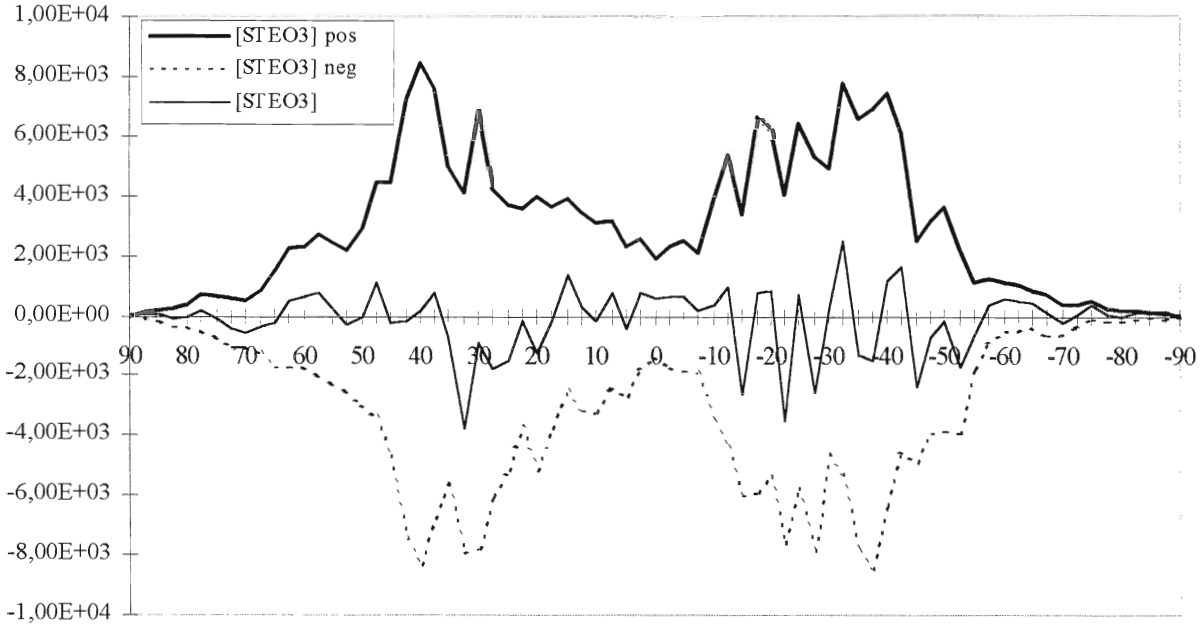

Figure 19: The sum of positive (upward) transport of ozone (thick line), the sum of negative (downward) transport of ozone (dotted line) and the net STE of ozone (thin line) for 14 December midnight. Values are in kgO_3 per second.

This particular example is representative for the other days applied in this study. At some latitudes, especially in the subtropics and midlatitudes, the net cross-tropopause ozone transport is almost zero while the total up- and downward transports are large. Small errors in the calculated total upward or total downward ozone transport can thus lead to large errors in the net ozone transport through the tropopause. These small errors can be caused by errors in the individual terms, as was argued above.

Gettelman et al. (1998) argued that even if the mass fluxes are heavily integrated over space and time, errors in the net mass transport can still be present. They found a mass imbalance over the course of a year when the mass flux was integrated over the entire globe. When the same integration was done for the mass flux across a pressure surface, the mass imbalance disappeared. By integrating the mass flux through a fixed pressure surface with the Wei method, only the vertical velocity in pressure co-ordinates (ω) remains in the flux formula. Therefore they concluded that the errors in the mass balance were not caused by biases in the vertical velocities. Instead it was argued that these errors are caused by systematic errors in the diagnosis of the PV surfaces. When a persistent bias is present in the nudging of the model temperatures towards observations, the PV is affected too. In

this way, the persistent bias could cause a systematic bias in the diagnosed mass flux through the tropopause. Gettelman et al. showed that even small errors in the calculated PV can lead to large errors in the cross-tropopause flux calculation. They concluded that quantitative information obtained from using the Wei method as applied to assimilated data sets should be interpreted with caution. The model data used in this study consist of assimilated meteorological fields too. The calculated PV values can therefore deviate from the PV values in the real atmosphere, giving cross-tropopause transports which may differ from real atmosphere cross-tropopause transports. But Gettelman et al. also stated that the Wei method is a useful tool when qualitative information about the mass flux across the tropopause is required. In case of this study, the Wei method is a useful tool for pinpointing the areas of zonal mean upward and downward transport of ozone through the tropopause.

In the near future, ozone observations will be assimilated in the ECMWF model and a longer, consistent ozone data set will be available. This future data set can be very useful for different climatological studies on the STE of ozone, for instance the regional dependency and the seasonal variability of the STE of ozone. In this respect, the present study can be seen as a first step it that direction with some preliminary results about the latitudinal dependency of the STE of ozone.

References

Andrews, D. G. and M. E. McIntyre, 1976, Planetary waves in horizontal and vertical shear: The generalized Eliassen-Palm relation and the mean zonal acceleration. *J. Atmos. Sci.* **33**, 2031-2048.

Angell, J., 1975, The field of mean vertical velocity at 200mb in south temperate latitudes as estimated from EOLE constant level balloon flights. *Quart. J. Roy. Meteorol. Soc.* **101**, 629-636.

Appenzeller, C., J. R. Holton and K. H. Rosenlof, 1996, Seasonal variation of the mass transport across the tropopause. *J. Geophys. Res.* **102**, 15071-15078.

Brewer, A. M., 1949, Evidence for a world circulation provided by the measurements of helium and water vapor distribution in the stratosphere. *Quart. J. Roy. Meteorol. Soc.* **75**, 351-363.

Cariolle, D. and M. Deque, 1986, Southern hemisphere medium-scale waves and total ozone disturbances in a spectral general circulation model. *J. Geophys. Res.* **91**, 10825-10846.

Danielsen, E. F. and V. A. Mohnen, 1977, Project Dustorm report: Ozone transport, in situ measurements and meteorological analyses of tropopause folding. *J. Geophys. Res.* **82**, 5867-5877.

Dobson, G. M. B., 1956, Origin and distribution of polyatomic molecules in the atmosphere. *Proc. Roy. Meteor. Soc.* **A236**, 187-193.

Fortuin, J. P. F. and U. Langematz, 1994, An update on the global ozone climatology and on concurrent ozone and temperature trends. In: *Atmospheric Sensing and Modelling,* ed. R. P. Santer, Proc. SPIE 2311, Washington DC, 207-216.

Gettelman, A. and A. H. Sobel, 1998, Direct diagnosis of stratosphere-troposphere exchange, submitted to: *J. Atmos. Sci.,* July 21, 1998.

Gettelman, A., J. R. Holton and K. H. Rosenlof, 1997, Mass fluxes of O_3, CH_4, N_2O and CF_2Cl_2 in the lower stratosphere calculated from observational data. *J. Geophys. Res.* **102**, 19149-19159.

Gidel, L. T., and M. A. Shapiro, 1980, General circulation model estimates of the net vertical flux of ozone in the lower stratosphere and the implication for the tropospheric ozone budget, *J. Geophys. Res.* **85**, 4049-4085.

Hoerling, M. P., T. K. Schaack and A. J. Lenzen, 1991, Global objective tropopause analysis. *Mon. Weather Rev.* **119**, 1816-1831.

Hoerling, M. P., T. K. Schaack and A. J. Lenzen, 1993, A global analysis of stratospheric-tropospheric exchange during northern winter. *Mon. Weather Rev.* **121**, 162-172.

Holton, J. R., 1992, *An Introduction to Dynamic Meteorology*, Academic Press.

Holton, J. R. and J. Lelieveld, 1996, Stratosphere-troposphere exchange and it's role in the budget of tropospheric ozone. In: *Clouds, chemistry and climate*, ed. P. J. Crutzen and V. Ramanathan, NATO ASI Series, Springer-Verlag, Berlin, 173-190.

Holton, J. R., P. H. Haynes, M. E. McIntyre, A. R. Douglass, R. B. Rood and L. Pfister, 1995, Stratosphere-troposphere exchange. *Rev. Geophys.* **33**, 403-439.

KNMI, RIVM, KMI, BIRA, 1997, Ozon en ultraviolette straling.

Levy II, H., 1971, Normal atmosphere: large radical and formaldehyde concentrations predicted. *Science* **173**, 141-143.

Mahlman, J. D., H. B. Levy and W. J. Moxim, 1980, Three-dimensional tracer structure and behaviour as simulated in two ozone precursor experiments. *J. Atmos. Sci.* **37**, 655-685.

Murphy, D. M. and D. W. Fahey, 1984, An estimate of the flux of stratosperic reactive nitrogen and ozone into the troposphere. *J. Geophys. Res.* **99**, 5325-5332.

Nastrom, G. D., 1977, Vertical and horizontal fluxes of ozone at the tropopause from the first year of GASP data. *J. Appl. Meteorol.* **16**, 740-744.

Roelofs, G. J. and J. Lelieveld, 1995, Distribution and budget of O_3 in the troposphere calculated with a chemistry general circulation model. *J. Geophys. Res.* **100**, 20983-20998.

Roelofs, G. J. and J. Lelieveld, 1997, Model study of the influence of cross-tropopause O_3 transport on tropospheric O_3 levels. *Tellus* **49B**, 38-55.

Satellite ozone data assimilation (SODA), 1997, 1st Annual report, ed. A. Stoffelen.

Shapiro, M. A., 1980, Turbulent mixing within a tropopause fold as a mechanism for the exchange of chemical constituents between the stratosphere and troposphere. *J. Atmos. Sci.* **37**, 994-1004.

Siegmund, P. C., P. F. J. van Velthoven and H. Kelder, 1996, Cross-tropopause transport in the extratropical northern winter hemisphere, diagnosed from high-resolution ECMWF data. *Quart. J. Roy. Meteorol. Soc.* **122**, 1921-1941.

Tie, X. X., and P. Hess, 1997, Ozone mass exchange between the stratosphere and troposphere for background and volcanic sulphate aerosol conditions. *J. Geophys. Res.* **102**, 25487-25500.

Vaughan, G., 1988, Stratosphere-troposphere exchange of ozone. In: *Tropospheric ozone,* ed. I. S. A. Isaksen, D. Reidel, Dordrecht, 125-135.

Wei, M,-Y., 1987, A new formulation of the exchange of mass and trace constituents between the stratosphere and the troposphere, *J. Atmos. Sci.* **44**, 3079-3086.

Wirth, V. and J. Egger, 1998, Diagnosing extratropical synoptic-scale stratosphere-troposphere exchange: a case study. Accepted by: *Quart. J. Roy. Meteorol. Soc.*

Yulaeva, E., J. R. Holton and J. M. Wallace, 1994, On the cause of the annual cycle in the tropical lower stratospheric temperature, *J. Atmos. Sci.* **51**, 169-174.

KNMI-PUBLICATIES, VERSCHENEN SEDERT 1995

Een overzicht van eerder verschenen publicaties, wordt verzoek toegezonden door de Bibliotheek van het KNMI, postbus 201, 3730 AE De Bilt, tel. 030 - 2 206 855, fax. 030 - 2 210 407; e-mail: biblioth@knmi.nl

KNMI-PUBLICATIE MET NUMMER

150-28 Sneeuwdek in Nederland 1961-1990 / A.M.G. Klein Tank
176-S Stormenkalender: chronologisch overzicht van alle stormen (windkracht 8 en hoger) langs de Nederlandse kust voor het tijdvak 1990-1996 / [samenst. B. Zwart a.o.]
180a List of acronyms in environmental sciences : revised edition / [compiled by P. Geerders and M. Waterborg]
181b FM12 SYNOP . internationale en nationale regelgeving voor het coderen van de groepen 7wwW1W2 en 960ww; derde druk
183-1 Rainfall in New Guinea (Irian Jaya) / T.B. Ridder
183-2 Vergelijking van zware regens te Hollandia (Nieuw Guinea), thans Jayapura (Irian Jaya) met zware regens te De Bilt / T. B. Ridder
183-3 Verdamping in Nieuw-Guinea, vergelijking van gemeten hoeveelheden met berekende hoeveelheden / T.B. Ridder
183-4 Beschrijving van het klimaat te Merauke, Nieuw Guinea, in verband met de eventuele vestiging van een zoutwinningsbedrijf / T.B. Ridder a.o.
183-5 Overzicht van klimatologische en geofysische publikaties betreffende Nieuw-Guinea / T.B. Ridder
184a Inleiding tot de algemene meteorologie : studie-uitgave ; 2e druk / B. Zwart, A. Steenhuisen, m.m.v. H.J. Krijnen
185a Handleiding voor het gebruik van sectie 2 van de FM 13-X SHIP-code voor waarnemers op zee / KNMI; KLu; KM
186-I Rainfall generator for the Rhine Basin: single-site generation of weather variables by nearest-neighbour resampling / T. Brandsma and T.A. Buishand
187 De wind in de rug: KNMI-weerman schaatst de Elfstedentocht / H. van Dorp

TECHNISCH RAPPORT = TECHNICAL REPORT (TR)

168 Analyse van het seismische risico in Noord-Nederland / Th. de Crook a.o.
169 Evaluatie van neerslagprognoses van numerieke modellen voor de Belgische Ardennen in december 1993 / Erik van Meijgaard
170 DARR-94 / C.P.G. Lomme
171 EFEDA-91: documentation of measurements obtained by KNMI / W.A.A. Monna a.o.
172 Cloud lidar research at the Royal Netherlands Meteorological Institute KNMI2B2, version 2 cloud lidar analysis / A.Y. Fong a.o.
173 Measurement of the structure parameter of vertical wind-velocity in the atmospheric boundary layer / R. van der Ploeg
174 Report of the ASGASEX'94 workshop / ed. by W.A. Oost
175 Over slecht zicht, bewolking, windstoten en gladheid / J. Terpstra
176 Verification of the WAQUA/CSM-16 model for the winters 1992-93 and 1993-94 / J.W. de Vries
177 Nauwkeuriger nettostraling meten / M.K. van der Molen en W. Kohsiek
178 Neerslag in het stroomgebied van de Maas in januari 1995: waarnemingen en verificatie van modelprognoses / R.Jilderda a.o.
179 First field experience with 600PA phased array sodar / H. Klein Baltink
180 Een Kalman-correctieschema voor de wegdektemperatuurverwachtingen van het VAISALA-model / A. Jacobs
181 Calibration study of the K-Gill propeller vane / Marcel Bottema
182 Ontwikkeling van een spectraal UV-meetinstrument / Frank Helderman
183 Rainfall generator for the Rhine catchment : a feasibility study / T. Adri Buishand and Theo Brandsma
184 Parametrisatie van mooi-weer cumulus / M.C. van Zanten
185 Interim report on the KNMI contributions to the second phase of the AERO-project / Wiel Wauben, Paul Fortuin a.o.
186 Seismische analyse van de aardbevingen bij Middelstum (30 juli 1994) en Annen (16 augustus '94 en 31 januari '95) / [SO]
187 Analyse wenselijkheid overname RIVM-windmeetlokaties door KNMI / H. Benschop
188 Windsnelheidsmetingen op zeestations en kuststations: herleiding waarden windsnelheden naar 10-meter niveau / H. Benschop
189 On the KNMI calibration of net radiometers / W. Kohsiek
190 NEDWAM statistics over the period October 1994 - April 1995 / F.B. Koek
191 Description and verification of the HIRLAM trajectory model / E. de Bruijn
192 Tiltmeting · een alternatief voor waterpassing ? / H.W. Haak
193 Error modelling of scatterometer, in-situ and ECMWF model winds; a calibration refinement / Ad Stoffelen
194 KNMI contribution to the European project POPSICLE / Theo Brandsma a.o.
195 ECBILT · a coupled atmosphere ocean sea-ice model for climate predictability studies / R.J. Haarsma a.o.
196 Environmental and climatic consequences of aviation: final report of the KNMI contributions to the AERO-project / W Wauben a.o.
197 Global radiation measurements in the operational KNMI meteorological network: effects of pollution and ventilation / F. Kuik
198 KALCORR: a kalman-correction model for real-time road surface temperature forecasting / A. Jacobs
199 Macroseismische waarnemingen Roswinkel 19-2-1997 / B. Dost e.a.
200 Operationele UV-metingen bij het KNMI / F. Kuik
201 Vergelijking van de Vaisala's HMP233 en HMP243 relatieve luchtvochtigheidsmeters / F. Kuik
202 Statistical guidance for the North Sea / Janet Wijngaard and Kees Kok
203 UV-intercomparison SUSPEN / Foeke Kuik and Wiel Wauben
204 Temperature corrections on radiation measurements using Modtran 3 / D.A. Bunskoek, A.C.A.P. van Lammeren and A.J. Feijt
205 Seismisch risico in Noord-Nederland / Th. De Crook, H.W. Haak en B. Dost
206 The HIRLAM-STAT-archive and its application programs / Albert Jacobs
207 Retrieval of aerosol properties from multispectral direct sun measurements / O.P. Hasekamp
208 The KNMI Garderen Experiment, micro-meteorological observations 1988-1989; instruments and data / F.C. Bosveld, J.G. van der Vliet and W.A.A. Monna.
209 CO2 in water and air during ASGAMAGE: concentration measurements and consensus data / Cor M.J. Jacobs, Gerard J. Kunz, Detlev Sprung a.o.
210 Elf jaar Cabauw-metingen / J.G. van der Vliet
211 Indices die de variabiliteit en de extremen van het klimaat beschrijven / E.J. Klok
212 First guess TAF-FGTAF: semi-automation in TAF production / Albert Jacobs
213 Zeer korte termijn bewolkingsverwachting met behulp van METCAST: een verificatie en beschrijving model-uitvoer / S.H. van der Veen
214 The implementation of two mixed-layer schemes in the HOPE ocean general circulation model/ M. van Eijk
215 Stratosphere-troposphere exchange of ozone, diagnosed from an ECMWF ozone simulation experiment / Harm Luykx

WETENSCHAPPELIJK RAPPORT = SCIENTIFIC REPORT (WR)

95-01 Transformation of precipitation time series for climate change impact studies / A.M.G. Klein Tank and T.A. Buishand
95-02 Internal variability of the ocean generated by a stochastic forcing / M.H.B. van Noordenburg
95-03 Applicability of weakly nonlinear theory for the planetary-scale flow / E.A. Kartashova
95-04 Changes in tropospheric NOx and O3 due to subsonic aircraft emissions / W.M.F. Wauben a.o.
95-05 Numerical studies on the Lorenz84 atmosphere model / L. Anastassiades
95-06 Regionalisation of meteorological parameters / W.C. de Rooy
95-07 Validation of the surface parametrization of HIRLAM using surface-based measurements and remote sensing data / A.F. Moene a.o.
95-08 Probabilities of climatic change : a pilot study / Wieger Fransen (ed.) a.o.
96-01 A new algorithm for total ozone retrieval from direct sun measurements with a filter instrument / W.M.F. Wauben
96-02 Chaos and coupling: a coupled atmosphere ocean-boxmodel for coupled behaviour studies / G. Zondervan
96-03 An acoustical array for subsonic signals / H.W. Haak
96-04 Transformation of wind in the coastal zone / V.N. Kudryavtsev a.o.
96-05 Simulations of the response of the ocean waves in the North Atlantic and North Sea to CO2 doubling in the atmosphere / K. Rider a.o.
96-06 Microbarograph systems for the infrasonic detection of nuclear explosions / H.W. Haak and G.J. de Wilde
96-07 An ozone climatology based on ozonesonde measurements / J.P.F. Fortuin
96-08 GOME validation at KNMI and collaborating institutes / ed. by P Stammes and A. Piters
97-01 The adjoint of the WAM model / H. Hersbach
97-02 Optimal interpolation of partitions: a data assimilation scheme for NEDWAM-4; description and evaluation of the period November 1995 - October 1996 / A.Voorrips
97-03 SATVIEW: a semi-physical scatterometer algorithm / J.A.M. Janssen a.o.
97-04 GPS water vapour meteorology · status report / H. Derks, H. Klein Baltink, A. van Lammeren, B. Ambrosius, H. van der Marel ao.
97-05 Climatological spinup of the ECBILT oceanmodel / Arie Kattenberg and Sybren S. Drijfhout
97-06 Direct determination of the air-sea transfer velocity of CO2 during ASGAMAGE / J.C.M. Jacobs, W. Kohsiek and W.A. Oost
97-07 Scattering matrices of ice crystals / M. Hess, P. Stammes and R.B.A. Koelemeijer
97-08 Experiments with horizontal diffusion and advection in a nested fine mesh mesoscale model / E.I.F. de Bruijn
97-09 On the assimilation of ozone into an atmospheric model / E.Valur Hólm
98-01 Steady state analysis of a coupled atmosphere ocean-boxmodel / F.A. Bakker
98-02 The ASGAMAGE workshop, September 22-25, 1997 / ed. W.A. Oost
98-03 Experimenting with a similarity measure for atmospheric flows / R.A. Pasmanter and X.-L. Wang
98-04 Evaluation of a radio interferometry lightning positioning system / H.R.A. Wessels
98-05 Literature study of climate effects of contrails caused by aircraft emissions / V.E. Pultau